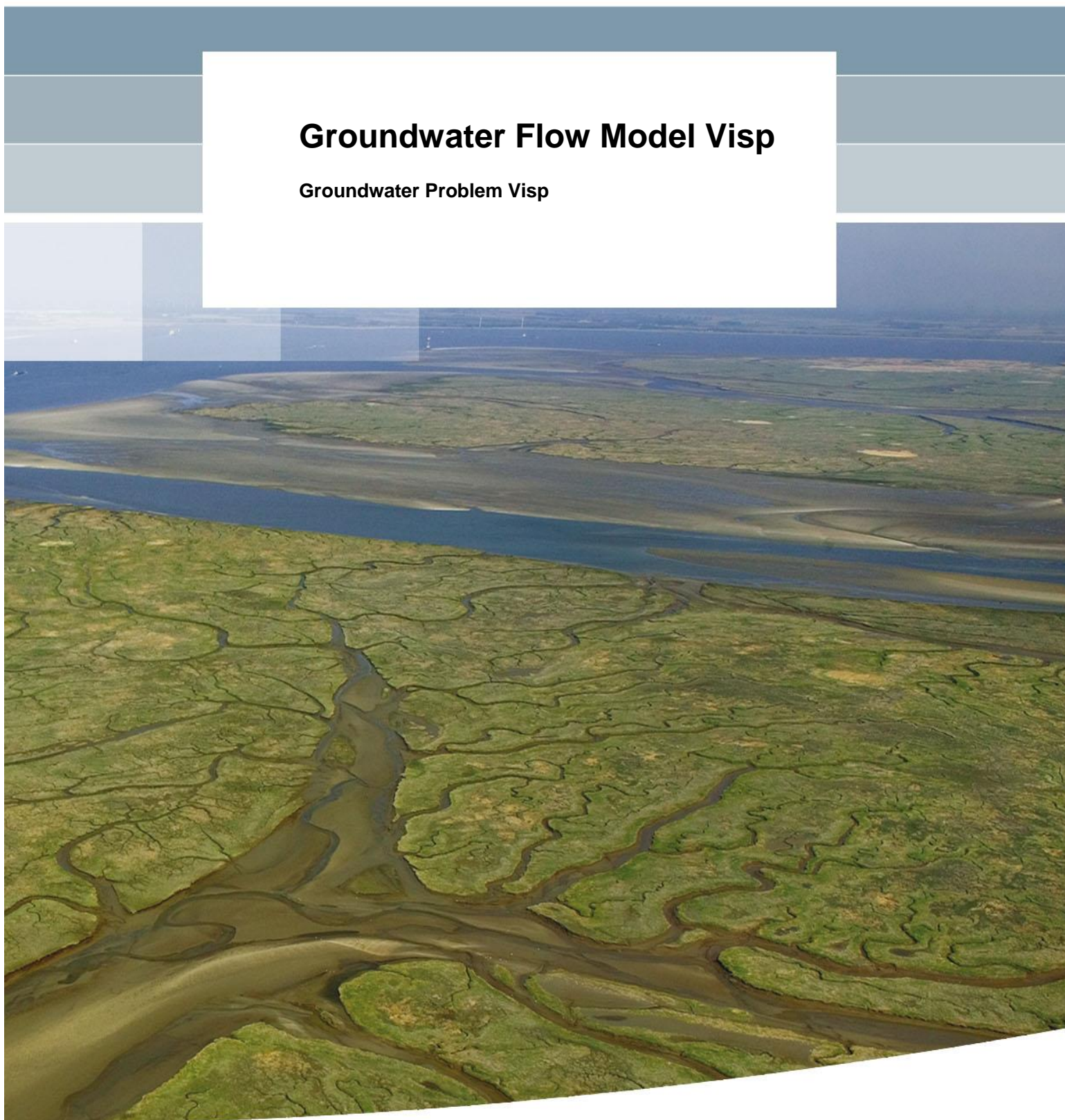


## **Groundwater Flow Model Visp**

**Groundwater Problem Visp**





# **Groundwater Flow Model Visp**

**Groundwater Problem Visp**

PTM Vermeulen

1220552-000





## Title

Groundwater Flow Model Visp

## Client

Geotechnisches Institut

## Project

1220552-000

## Reference

1220552-000-BGS-0001

## Pages



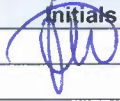
47

## Keywords

Visp, Groundwater, Surface- and groundwater interaction, iMOD

## Summary

Since December 2011, the municipality of Visp, faces abnormally high groundwater levels. In close collaboration with the authorities of Canton Valais, the municipality of Visp decided to initiate in 2014 a detail investigation of the causes behind these extraordinary groundwater levels. This report describes in this context the construction of a transient, three-dimensional groundwater flow model of the extended Visp basin to closer evaluate the effects of the extraction wells of Lonza Industry, the river stages in the Vispa and Rhône River as well as the effect caused by the underground infrastructures in Visp.

Version	Date	Author	Initials	Review	Initials	Approval	Initials
	Oct. 2015	P.T.M. Vermeulen		W. Borren		H. Duel	

## State

final



## Contents

<b>1 Introduction</b>	<b>7</b>
1.1 Motivation	7
1.2 Study Area	7
1.3 Topography	8
1.4 Time	8
<b>2 Geology</b>	<b>9</b>
2.1 Introduction	9
2.2 Boreholes and hard-rock	10
2.3 Subsoil modelling and parameterisation	12
<b>3 Model Input</b>	<b>17</b>
3.1 Groundwater Recharge	17
3.2 Boundary Conditions	19
3.2.1 Fixed Potential Boundary	20
3.2.2 Closed Model Boundary	21
3.2.3 Fixed Flux Boundary	22
3.3 Groundwater level Observations	22
3.4 Initial Groundwater level	23
3.5 Surface Water	24
3.5.1 Rhône River	24
3.5.2 Vispa River	25
3.5.3 Rhône and Vispa Rivers	26
3.6 Groundwater Extractions	27
3.7 Cellars	29
<b>4 Optimization</b>	<b>31</b>
4.1 Introduction	31
4.1.1 Optimization with parameter set 1	31
4.1.2 Optimization with parameter set 2	32
4.1.3 Optimization with parameter set 3	32
4.1.4 Optimization with parameter set 4	33
4.2 Model Results	35
4.2.1 Groundwater levels	35
4.2.2 Water balance of the entire model	38
<b>5 Scenarios</b>	<b>41</b>
5.1 Initial scenarios	41
5.1.1 Introduction	41
5.1.2 Results	41
5.2 Additional scenarios	41
5.2.1 Introduction	41
5.2.2 Results	44
<b>6 Summary and recommendations</b>	<b>47</b>
<b>7 References</b>	<b>49</b>

## Appendices

### A Drawdown of Scenarios

A-1

## List of Tables

Table 2.1	Lithological Units and Geohydrological Units.....	10
Table 2.2	Initial parameter set for permeability values in the Rhône (R) and Vispa (V) valley, blue are the water bearing model layers.....	12
Table 3.1	Averaged infiltration factors per month. ....	17
Table 3.2	Example of the computation of the time varying groundwater recharge. ....	18
Table 3.3	Estimated water levels in the Rhône for the model area. ....	25
Table 3.4	Estimated water levels in the Vispa for the model area.....	26
Table 3.5	Existing extraction locations and corresponding rates nearby Visp for different categories. ....	28
Table 4.1	Optimization results for the first set of three parameters.....	31
Table 4.2	Optimization results for the second set of four parameters.....	32
Table 4.3	Optimization results for the third set of five parameters.....	32
Table 4.4	Optimization results for the fourth set of seven parameters.....	33
Table 4.5	Computed parameter confidence intervals (96%). Parameter abbreviations as used in Table 4.1 to 4.4.....	35
Table 4.6	Computed water balance for the entire model area.....	38
Table 5.1	Results for the additional scenarios. ....	45



## List of Figures

Figure 1.1	E-W view of the Model Area with the location of the city of Visp, and the rivers Rhône and Vispa in the model. ....	8
Figure 2.1:	Aquifer structure between Baltschieder and Gamsen, (Kimmeier, 2001) .....	9
Figure 2.2	Three-dimensional presentation of the existing boreholes coloured by their lithology.....	11
Figure 2.3	Three-dimensional presentation of the existing boreholes coloured by their units of geohydrology.....	11
Figure 2.4	Estimated depth of the hard-rock in the Rhône- and Vispertal (data after Rosseli & Olivier, 2003).....	12
Figure 2.5	Cross-section over the model area from west to east with the digitized interfaces for the model layers.....	13
Figure 2.6	The upper-most detail of a cross-section depicted in Figure 2.5 over the model area from west to east with boreholes projected perpendicular on the cross-section. ....	14
Figure 2.7	Three-dimensional image of the cross-sections that were developed to construct the subsoil solid. ....	14
Figure 2.8	Three-dimensional image of the subsoil. ....	15
Figure 3.1	Measured daily precipitation for (left) Visp and (right) Grächen in mm/day. ....	17
Figure 3.2	Estimated distinction in rural (green) and urban (red) areas. ....	18
Figure 3.3	Estimated groundwater recharge (mm/day) for the rural areas.....	19
Figure 3.4	Model area and the layout of the chosen model boundaries.....	19
Figure 3.5	Locations for the selected observation wells for the boundary conditions. ....	20
Figure 3.6	Scatter plots of the measured observations for the boundary conditions, (left) VSB37-PZ15, (middle) VD75-VD10 and (right) VH45-VZ01. ....	21
Figure 3.7	Times series for the observation wells of the fixed potential boundary conditions.....	21
Figure 3.8	Layout of the six sub catchment areas that discharge directly into the aquifer of the Rhône valley.....	22
Figure 3.9	Location of the six observation wells used for quality-control of the model and the averaged values for calibration purposes. ....	23
Figure 3.10	Times series for the observation wells for calibration. ....	23
Figure 3.11	Interpolated groundwater level (Kriging) for the 1 <sup>st</sup> of February 2011. ....	24
Figure 3.12	Measured water levels at MQA, filled in partly with measures from station 2346 (Brig). ....	25
Figure 3.13	Measured water levels at station 2351.....	26
Figure 3.14	Three-dimensional representation of the computed water levels for the Rhône and Vispa River. ....	27



Figure 3.15	Location of extraction wells for drinking (Hohbrunnen/Katzenhaus) and industrial use (Lonza, 4 distinctive wells). ....	27
Figure 3.16	Location of selected extraction wells for artificial recharge and other usages. ....	28
Figure 3.17	Measured extraction rate in m <sup>3</sup> /day for the Lonza Industry between 2010 and 2014. ....	29
Figure 3.18	Measured extraction rate in m <sup>3</sup> /day for the Drinking water supply for the municipality of Visp between 2011 and 2013. ....	29
Figure 3.19	Overview of the major underground infrastructures ("elements") in the city of Visp, coloured by their estimated depth in meter below surface level (source: Municipality of Visp) .....	30
Figure 3.20	Cross-section showing the penetration of the elements depicted in Figure 3.19. ....	30
Figure 4.1	Computed versus measured groundwater levels for VH45 in Visp: a) the original results prior to the optimization; b) three parameters; c) four parameters; d) five parameters and e) seven parameters .....	33
Figure 4.2	Computed (orange) and measured (green) groundwater levels for all observation wells. ....	34
Figure 4.3	Computed statistics (left) before the parameter optimization and (right) thereafter.....	35
Figure 4.4	Computed groundwater level in the first aquifer (model layer 2) for top) 1 <sup>st</sup> of January 2012, middle) 3 <sup>rd</sup> of July 2012 and bottom) 1 <sup>st</sup> of January 2013.....	36
Figure 4.5	Computed depth of the groundwater table (model layer 1) for top) 1 <sup>st</sup> of January 2012, middle) 3 <sup>rd</sup> of July 2012 and bottom) 1 <sup>st</sup> of January 2013.....	37
Figure 4.6	Definition of the water balance items. See also Figure 3.4 for the definition of the chosen model boundaries.....	38
Figure 5.1	(top) Time series of the computed groundwater levels in VH45 in Visp; (bottom) the differences between the scenarios and the reference time series.....	42
Figure 5.2	Side flow for (green) the original situation and (red) the scenario whereby this side flow is reduced for 75% and (blue) the situation whereby the side flow is reduced by 50% for the Vispa valley only. ....	43
Figure 5.3	(top) The time series of the original river stage (blue) and 2011 sequence applied to 2012 for the Rhône and (bottom) the time series of the original river stage (red) and 2011 sequence applied to 2012 for the Vispa River (blue). ....	43
Figure 5.4	(top) time series of the (blue) original Hohbrunnen extraction and (green) the extraction regime of 2011 projected to 2012; (bottom) time series of the (green) original Lonza extraction (Sandmatten B1) and (blue) the extraction regime of 2011 projected to 2012.....	44
Figure 5.5	(top) time series of the (red) original groundwater level at Staldbach and (blue) the groundwater level of 2011 projected to 2012; (bottom) time series of the (blue) original groundwater level at Lalden and (red) the groundwater level of 2011 projected to 2012.....	44
Figure 5.6	Simulated time series of the differences for the scenarios SN1 up to SN6. ....	45

# 1 Introduction

## 1.1 Motivation

Since December 2011, the municipality of Visp faces abnormally high groundwater levels. In the high-water period of 2013, some private cellars in the Southern part of the city have been reported infiltrated by groundwater. On this occasion, the authorities of Canton Valais and the municipality of Visp have initiated a collaboration to address this groundwater management issue from a more global perspective. In this framework, the Geotechnisches Institut AG has been assigned to conduct a detailed expertise. As part of the study, the Environmental protection Agency of Canton Valais proposed to develop a transient, three-dimensional groundwater flow model of the extended Visp basin, which should help better understanding the aquifer systems and the overall water balance. The model was proposed to be built in collaboration with Deltares using iMOD software (Vermeulen, 2015). Accordingly, an exhaustive data set has been sent to Deltares on 23<sup>rd</sup> of November 2014 together with the model concept defined by Geotechnisches Institut.

One of the main goals of the study is therefore to clarify if whether or not the cause of the high groundwater levels observed in 2013 has a natural (i.e. effects of climate change in an alpine environment) or manmade origin (i.e. unsustainable land use/construction practices). In particular, this model reports the differences between the measured and the computed groundwater heads for three indicative periods (1<sup>st</sup> of January 2012, 3<sup>rd</sup> of July 2012 and 1<sup>st</sup> of January 2013). Furthermore a water balance is presented in a time-graph showing the different balance items in the model. For the various modelling scenarios, time series are each time presented for the measurement location VH45 in Visp, in combination with the original head from the reference scenario.

## 1.2 Study Area

The study area is part of the alluvial plain of the upper Rhône River and coincides with the political boundaries of the Swiss Canton of Valais (Glenz, 2013). The groundwater of the alluvial aquifer plays an important economic role; it is used for drinking, industrial, geothermal and irrigation purposes (fruit-growing, market gardening). The study area is approximately  $10 \times 5 = 50 \text{ km}^2$ , see Figure 1.1. The model is constructed in the CH1903 (LV03) coordinate system. All files implemented by the iMOD groundwater flow model are to be saved in this coordinate system to ensure consistency. The final resolution of the entire model is  $10 \times 10 = 100 \text{ m}^2$  in Visp.

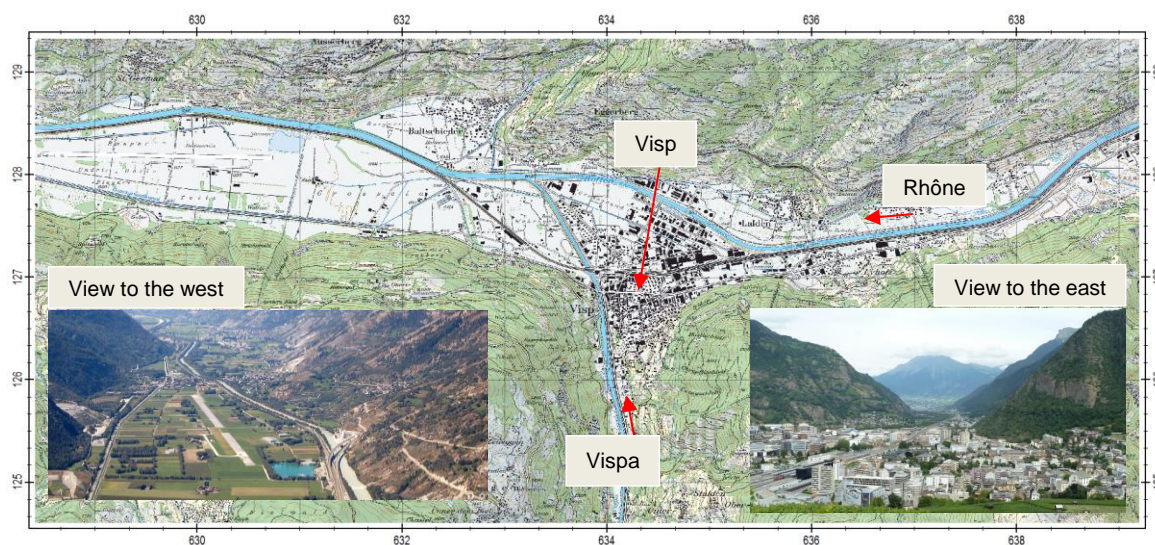


Figure 1.1 E-W view of the Model Area with the location of the city of Visp, and the rivers Rhône and Vispa in the model.

### 1.3 Topography

The topography is typical for an alpine system in that it presents a strong relief between high mountains ranging up to more than 4000 m and the alluvial plain, which has a mean altitude of 635 in the west and 660 m in the east of study area. To the south of Visp, the altitude rises in the Vispental up to about 700 m.

### 1.4 Time

The groundwater flow in and around Visp is simulated for a steady-state and a transient period. The steady-state simulation is based on groundwater levels that are meant to be representative for an undefined period without taking into account the effect of the seasonal variations. The transient simulation highlights the dynamics of the groundwater levels on a daily basis for the period between the 1<sup>st</sup> of February 2011 and the 31<sup>st</sup> of December 2013. The actual period for analyses is the 2<sup>nd</sup> of February 2012 and the 31<sup>st</sup> of December 2012.

## 2 Geology

### 2.1 Introduction

The Rhône plain forms a huge *bowl* filled with Quaternary sediments, the thickness of which reaching almost 1000 m in place (Besson *et al.*, 1993). At depth, several aquifer layers of various thickness and geochemical signature are depicted. The top layer essentially consists of fluvial deposits of the Rhône River. Also found are glacial deposits, torrential deposits (alluvial fan during the water side) and slope deposits (talus). Based on the large number of data collected by Fröhlich (1997) between Baltschieder and Gamsen near Visp, the region is basically composed out of two main geological units, namely:

- **Bedrock:** Bedrock can already be reached at a depth of about 100 m as documented by borehole data in Brigerbad near Brig. However the depth of the bedrock near Visp is generally expected to be much deeper, around 500 meters and more (Rosselli & Olivier, 2003). With increasing depth, hydrothermal groundwater circulation is expected to be found at the contact between the bedrock and the Quaternary deposits. Despite of some direct evidences through borehole operations, the geometry and extent of the geothermal reservoir is still highly speculated.
- **Quaternary Deposits:** Quaternary deposits consist primarily of fluvial (river) and lacustrine (lake) sediments inherited from the last glaciation period. The fluvial deposits consist mainly of sandy gravel or sandy loam with a variable proportion of stones and blocks. The Quaternary deposits are river alluvium (unconsolidated) usually topped by flood deposits (silts) which thickness varies considerably from place to place (0.10 – 10 meter). Those sediments form lenses with axes generally parallel to the direction of the Rhône River. They constitute the largest formation of the alluvial Rhône valley. According to Kimmeier (2001), different intercalated layers of this deposit are found which divide the alluvium in two different sub levels, see Figure 2.1.

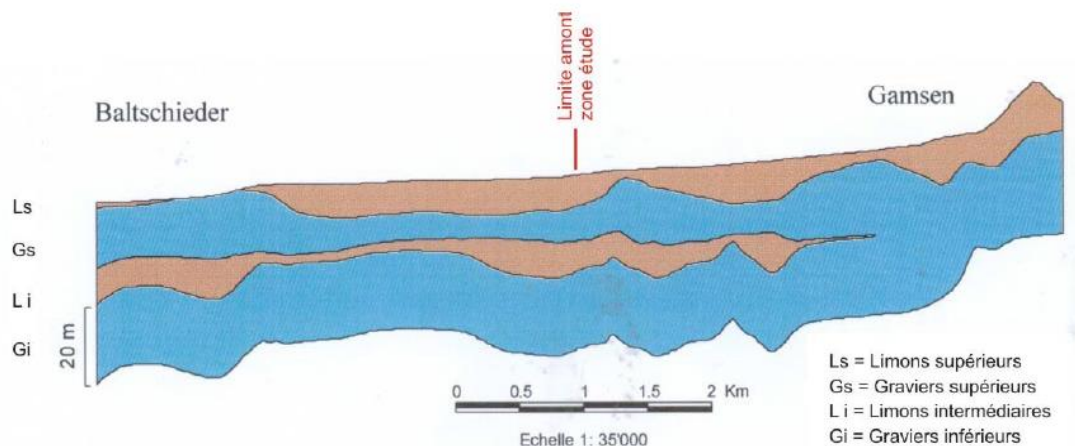


Figure 2.1: Aquifer structure between Baltschieder and Gamsen, (Kimmeier, 2001)

The aquifer system proposed by Kimmeier (2001) can be summarized by a sequence of 4 lithological formations as:

1. **LS:** Surface flood deposits with an average thickness of 10 meter, which may be absent in places;
2. **GS:** Upper gravels with an average thickness of 16 m;

3. LI: Intermediate flood deposits, which have a maximum thickness of 20 m and which can be absent in places;
4. GI: Lower gravels for which the thickness is not well known because an evident lack of borehole data at those depths.

This subdivision is however not found everywhere and differences between the left and the right banks of the river were found as well. The lateral limits of the aquifer are represented by the slopes side of the bedrock that have been inferred from gravimetric measurements (Rosselli & Olivier, 2003).

Recent borehole data suggest that the aquifer geometry under Visp might be more complex than previously recognized. This is particularly well documented by a recent drilling campaign of ETHZ that crossed 4 distinctive aquifer layers on a vertical section of 100 m (COGEAR-Project, 2015). These recently obtained direct evidences of the underground structure below Visp permit to refine the conceptual model and highlight the local heterogeneity.

The region also shows hydrothermal activity with evidence of a deep seated groundwater circulation through the bedrock and concurrent interaction with the Quaternary deposits.

## 2.2 Boreholes and hard-rock

In the model the underground structure will be discretised up to the hard-rock (bedrock), based on the borehole data as provided by Canton Valais (SPE with the support of CREALP). Only the main lithologies (sand and clay) with a significant extent will be distinguished. The distinguished lithology and geohydrological units are presented in Table 2.1. It should be noted that similar lithologies can have different geohydrological units, in other words, the flood deposits (FloD) are mainly containing low permeable material (DKL) however, in parts of the area those FloD lithologies have high permeable materials (FGW).

Table 2.1 Lithological Units and Geohydrological Units.

Lithology Code	Description	Geohydrological Units	Description
BaF	Backfill (artificial)	FGW	Water-bearing subsurface layer (free groundwater)
FloD	Flood Deposits	DKL	Low permeable subsurface layer (cover of a confined or semi-confined aquifer)**
FluvD	Fluvial Deposits	WBL	Water-bearing layer
SwaD	Swampy Deposits	SDL	Low permeable layer
GlaD	Glacial Deposits	BAS	Base of the porous aquifer; a constant flux boundary assumed (poorly constrained hydrothermal groundwater circulation)
PaIS	Paleosol		
BR	Bedrock		

The boreholes are depicted in Figure 2.2 according to their lithology. The flood deposits and fluvial deposits are clearly observable, as well as the swampy deposits. The flood deposits are disappearing to the west in the area of Gamsenried, as depicted in the conceptual image in Figure 2.1 as well.



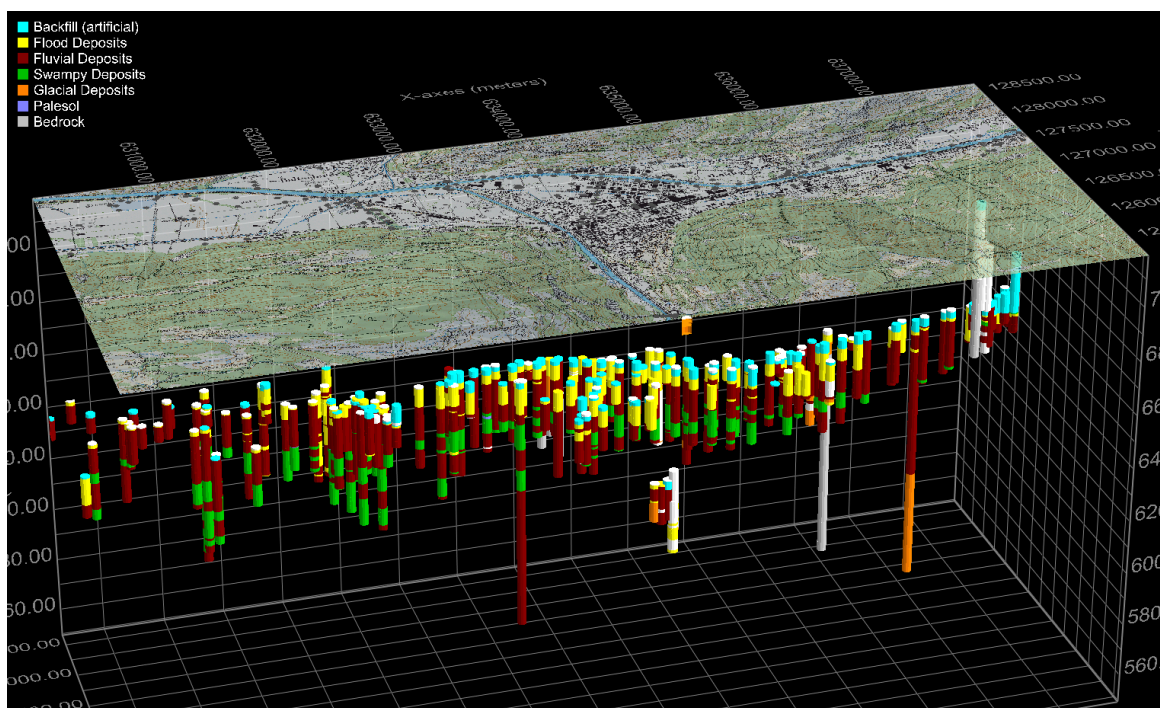


Figure 2.2 Three-dimensional presentation of the existing boreholes coloured by their lithology.

The water bearing capability of the different lithologies has been presented in Figure 2.3. To the west there is an unconfined water bearing layer, whereas the aquifer is confined to the east.

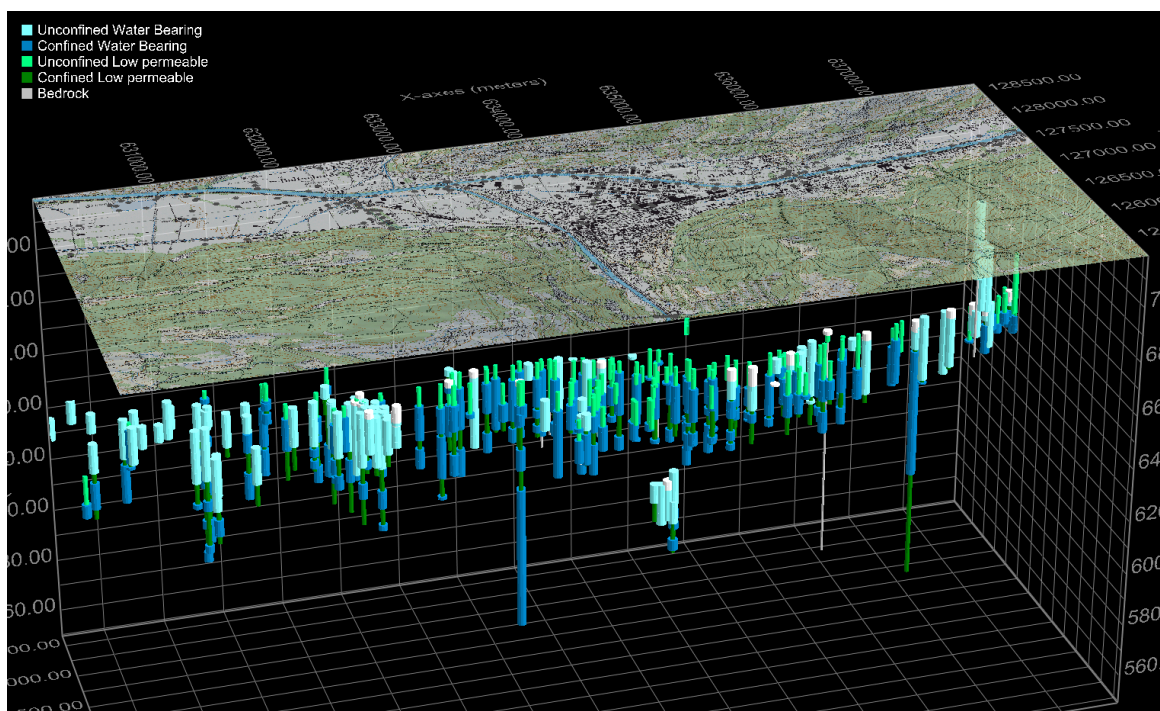


Figure 2.3 Three-dimensional presentation of the existing boreholes coloured by their units of geohydrology.

From Figure 2.3 it can be seen that there is a clear subdivision of several water-bearing layers (blue colours) divided by layers with lower permeability's (green colours).

The bottom of the model corresponds to the hard-rock (bedrock) that shows a significant vertical extent and is assumed filled in with poorly sorted glacial deposits. The estimated depth of the hard-rock based on gravimetric measurements (Rosseli & Olivier, 2003) has been depicted in Figure 2.4. The depth of the Rhône valley reaches up to 550 meter whereas the depth to the hard-rock in the Vispताल is less than 50 meters only. The Rhône valley is filled in with coarse, well sorted material on top and this becomes less sorted downwards. The Vispताल has been filled in with well-sorted fluvial deposits.

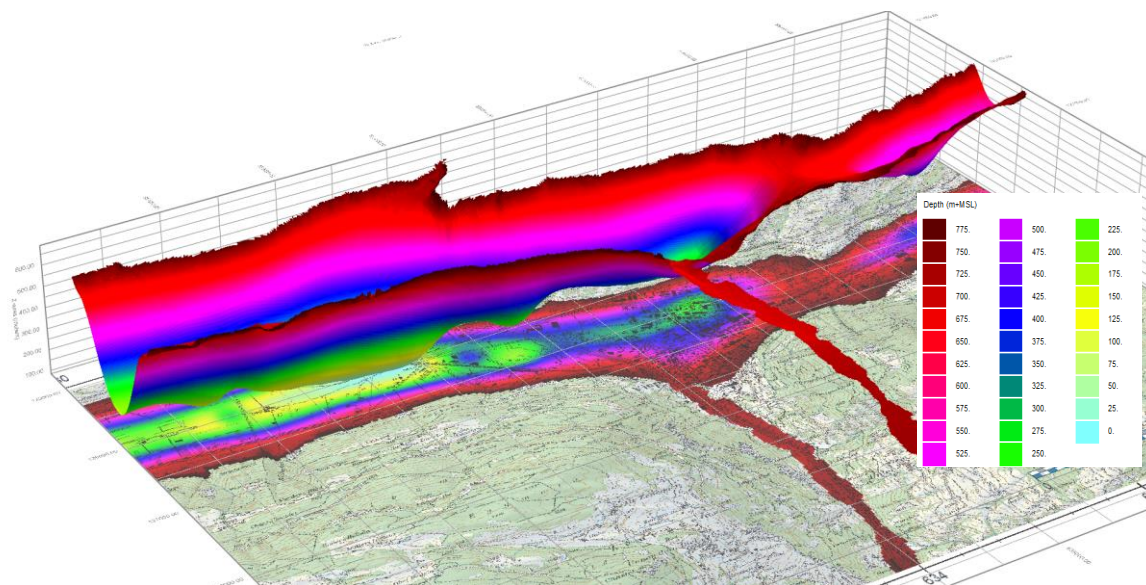


Figure 2.4 Estimated depth of the hard-rock in the Rhône- and Vispताल (data after Rosseli & Olivier, 2003).

## 2.3 Subsoil modelling and parameterisation

In the Solid Tool of iMOD (Vermeulen, 2015), the water-bearing intervals interpreted from the boreholes were used to construct a three-dimensional solid of the subsoil. Here fore, the main water-bearing horizons with a significant extent were connected. Minor inclusions of water-bearing bodies were excluded to be a separate layer in the model. A total of 6 model layers were identified. In Table 2.2 the initial parameters are given as well as the definition and description of the several model layers.

Table 2.2 Initial parameter set for permeability values in the Rhône (R) and Vispa (V) valley, blue are the water bearing model layers.

Model layer	R/V	Description	Averaged Permeability (m/s)	Initial Permeability (m/d)	Min. value (m/d)	Max. value (m/d)	Opt. N=no Y=Yes
1	R	Flood deposits	$1.16E^{-6}$	0.1	-	-	N
2	R	Fluvial deposits	$1.45E^{-3}$	125.0	60.0	432.0	Y
	V		$1.16E^{-3}$	50.0	45.0	175.0	Y
3	R	Swamp deposits	$1.16E^{-6}$	0.1	-	-	N
4	R	Fluvial deposits	$1.45E^{-3}$	125.0	86.4	432.0	Y
	V		$0.58E^{-3}$	50.0	45.0	175.0	Y
5	R	Swamp deposits	$1.16E^{-6}$	0.1	-	-	N



Model layer	R/V	Description	Averaged Permeability (m/s)	Initial Permeability (m/d)	Min. value (m/d)	Max. value (m/d)	Opt. N=no Y=Yes
6	R	Glacial Deposits	$1.16\text{E}^{-4}$	10.0	-	-	N
	V	Fluvial deposits	$0.58\text{E}^{-3}$	50.0	45.0	175.0	Y

The fluvial deposits are well sorted and have a high permeability value; the initial permeability for those gravels is 125 m/day ( $1.45\text{E}^{-3}$  m/s) in the Rhône valley and permeability values of 50 m/day ( $0.58\text{E}^{-3}$  m/s) in the Vispental. During the parameter optimization (see section 4.1), a bandwidth is applied in which the permeability may increase or decrease up to almost a factor 2. The low permeable material (flood- and swampy deposits) have significant lower permeability values, estimated at 0.1 m/day. Finally, the deep, glacial deposits, consists out of poorly sorted material and has a low permeability of 10.0 m/day ( $1.16\text{E}^{-4}$  m/s). This material doesn't occur in the Vispental, therefore within model layer 6 the material consists out of fluvial deposits as well.

The effective porosity is estimated to be 12%, meaning that 12% of the material of the subsoil could contain water. For the deeper water-bearing layers, the initial specific storage coefficient is  $1\text{E}^{-4}$  up to  $7\text{E}^{-4}$  m<sup>-1</sup>. This determines the amount of water that can be stored in the subsurface by an increase of water pressure. These parameters will be optimized in the parameter optimization (see section 4.1).

The Solid Tool of iMOD makes it possible to construct a solid of the subsoil by means of cross-sections in which the interfaces for the model layers are defined. The creation of the solid starts with a rough delineation of the interfaces to capture the global pattern of deposits in the valley. From there, more detail can be easily included.

In Figure 2.5, a W-E cross-section of the model area is presented. In the direct vicinity of Visp the depth of the hard-rock ranges from > 200 m to > 500 m. The hard-rock declines from west to east up to a depth of less than 50 meter. The majority of the boreholes penetrate the subsoil up to a depth of 25-50 meter, with only few data to greater depths.

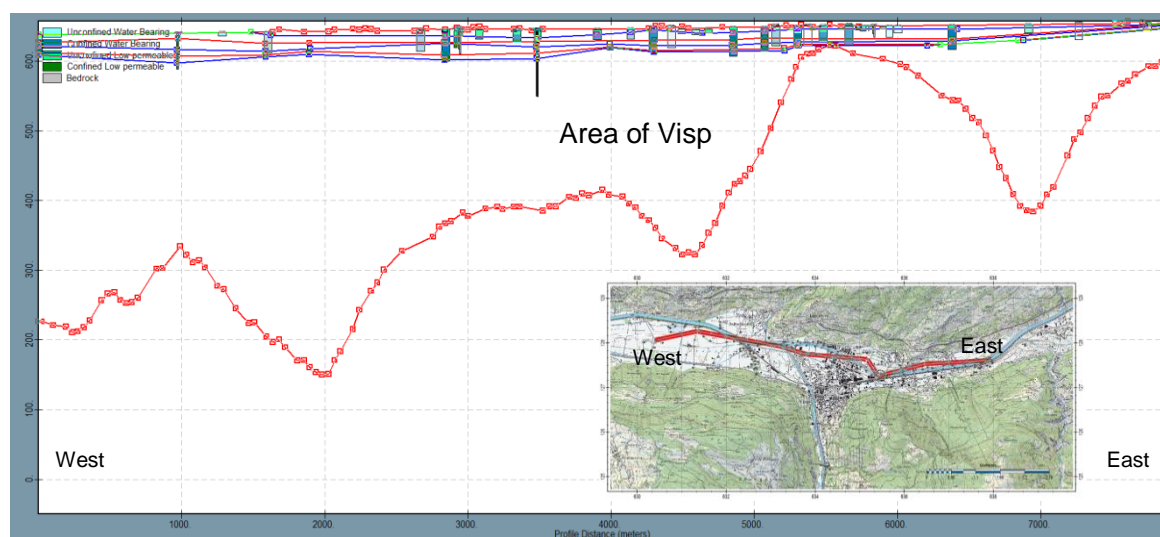


Figure 2.5 Cross-section over the model area from west to east with the digitized interfaces for the model layers.

It is assumed that no separated water-bearing layers can be distinguished deeper than 50 meter below the surface. Deeper than 50 m, it is therefore assumed (based on the few available data) that the deposits are poorly sorted and no distinction can be made in separate water-bearing layers and clayey layers.

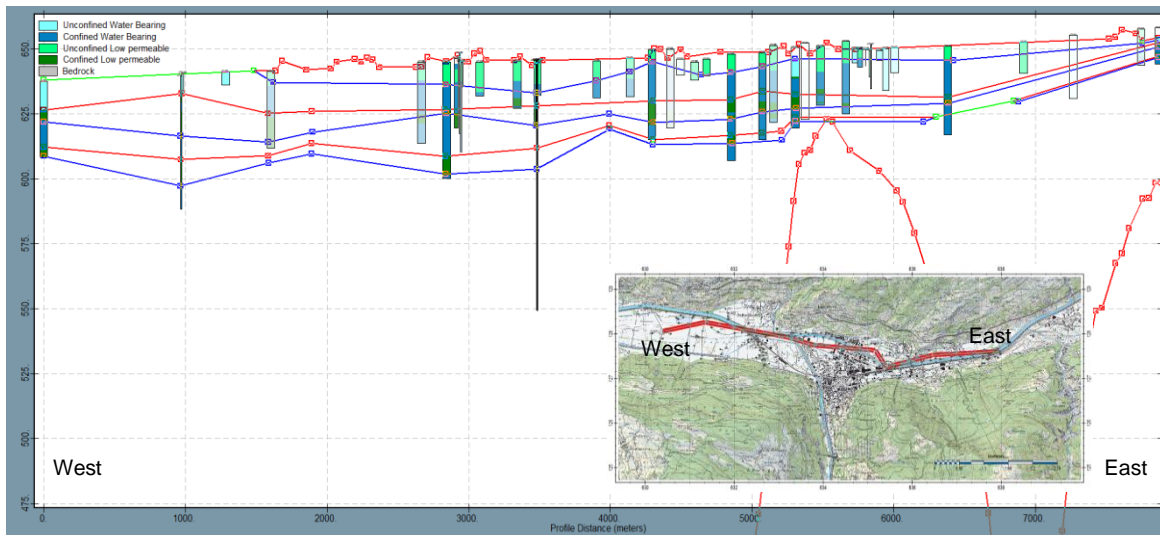


Figure 2.6 The upper-most detail of a cross-section depicted in Figure 2.5 over the model area from west to east with boreholes projected perpendicular on the cross-section.

In Figure 2.6, a detail is presented for the upper most part of the cross-section as presented in Figure 2.5. The lighter the borehole is displayed, the further away the borehole is positioned perpendicular to the cross-sections. In the cross-section the interfaces are displayed, whereby the red lines represent the top of each low permeable layer, the blue lines indicate the top of the water-bearing layers. A green line represents the absence of a clayey layer. In 10 cross-sections, the interfaces for the water-bearing- and clayey layers are delineated, see Figure 2.7.

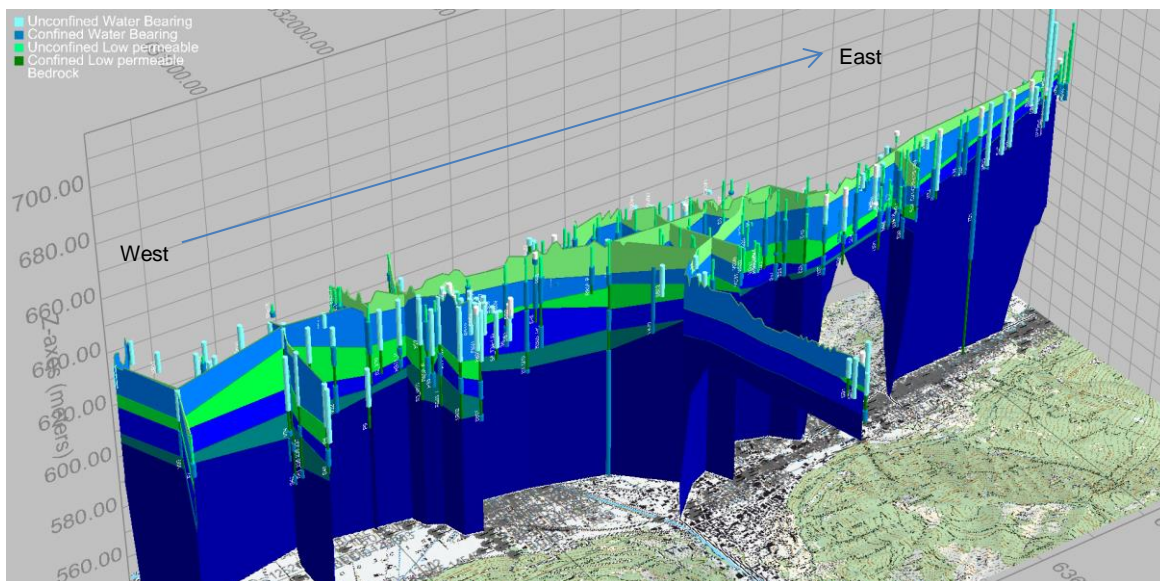


Figure 2.7 Three-dimensional image of the cross-sections that were developed to construct the subsolid.

At each intersection between the cross-sections, the interfaces are equalized to avoid any abrupt offset. As can be clearly seen, there is no clayey material in the Vispental, other than some minor appearances at the end. Finally, those interfaces are interpolated to a spatial three-dimensional representation of the subsoil, see Figure 2.8.

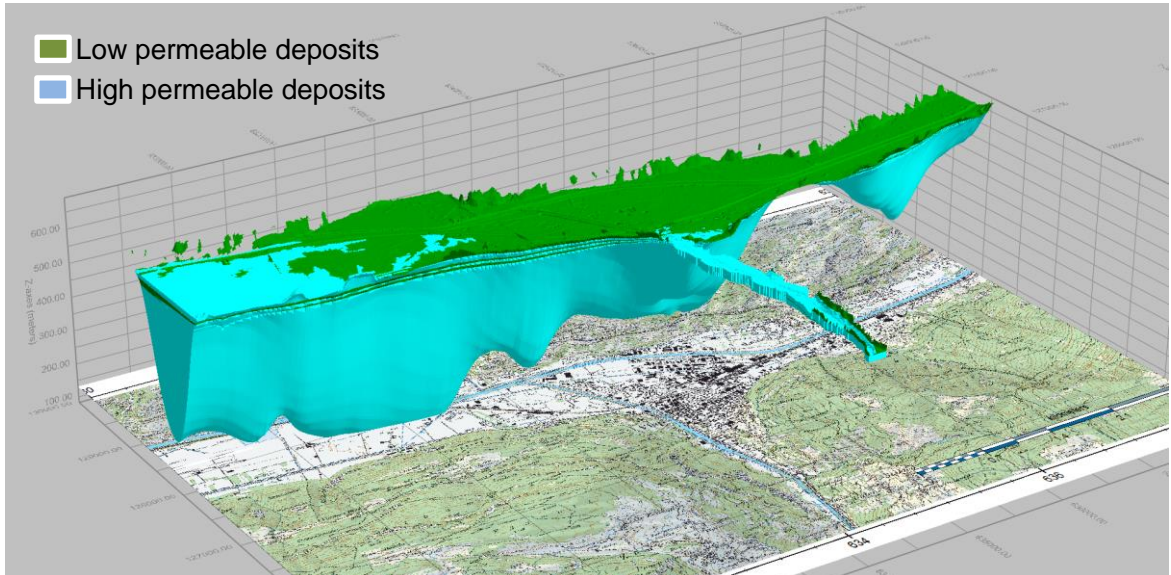


Figure 2.8 Three-dimensional image of the subsoil.

The subsoil clearly shows the absence, in the western part of the Rhone valley and the Vispental, of the first layer with low permeable material. The first water-bearing model layer outcrops directly to the surface level as this layer is covered by a layer with low permeable material in- and around Visp.

Those interfaces, together with the permeability's per model layers form the conductances of the subsoil. The respective values determine the “easiness” of groundwater to flow into particular directions, horizontally and/or vertically.



### 3 Model Input

#### 3.1 Groundwater Recharge

The valley of Visp is – relative to the rest of Switzerland – extremely dry as it receives an annual average precipitation of only 575 mm/year, i.e. 1.58 mm/day. The mountains around Visp receive a bit more precipitation and the rain gauge of Grächen is therefore assumed to be more representative for the prevalent hydrological regime. The measured precipitation for both rain gauges is presented in Figure 3.1.

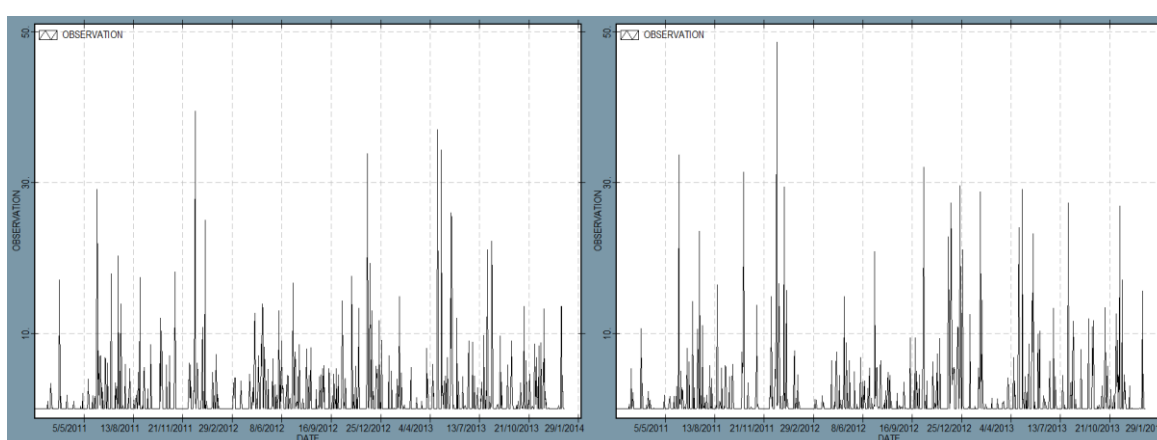


Figure 3.1 Measured daily precipitation for (left) Visp<sup>1</sup> and (right) Grächen in mm/day.

Groundwater Recharge (R) refers to the surplus of precipitation that seeps through the subsoil and feeds the volume of groundwater. This surplus relates to the characteristics of the unsaturated zone, climate (Precipitation P), vegetation (EvapoTranspiration ET) and urban areas (Interception I), so:

$$R = P - ET - I$$

The unsaturated zone causes a time-delay and spread out between the moment of precipitation and the actual recharge of the groundwater. This time-delay and spread out are modelled by computing the moving average of the precipitation P for 5 days. Evapotranspiration ET by vegetation is higher in summer than in winter times. In the model ET relates to the Precipitation by a time varying infiltration factor F that takes into account the seasonal variability, see Table 3.1.

Table 3.1 Averaged infiltration factors per month.

Jan.	Feb.	March	April	May	June	July	Aug.	Sept.	Oct.	Nov.	Dec.
80%	70%	50%	30%	10%	5%	5%	5%	10%	30%	70%	80%

The final groundwater recharge is subdivided in a rural and urban area. In urban area a 50% reduction is applied due to a high level of built-up area in the city centre of Visp and the industrial areas see Figure 3.2.

<sup>1</sup> No measurements were available for the periods 5<sup>th</sup> of August 2012 – 13<sup>th</sup> of August 2012 and 1<sup>st</sup> of December 2013 – 4<sup>th</sup> of December 2013.



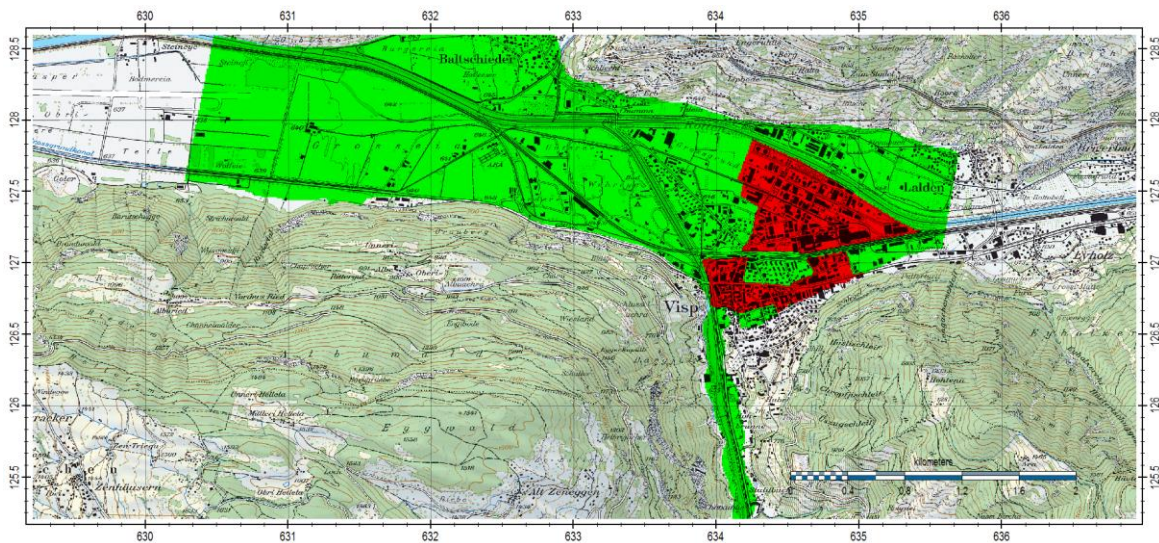


Figure 3.2 Estimated distinction in rural (green) and urban (red) areas.

As an example, the above described methodology has been written out for a short period 1<sup>st</sup> of January 2013 up to the 7<sup>th</sup> of January 2013 and depicted in Table 3.2.

Table 3.2 Example of the computation of the time varying groundwater recharge.

Date	Precipitation P (mm/day)		Infiltration Factor F	Recharge R (mm/day)	
	Daily Sum	Moving Average		Rural Area	Urban Areas 50%
1-1-2013	0.0				
2-1-2013	0.0				
3-1-2013	0.0				
4-1-2013	0.0				
5-1-2013	3.0				
6-1-2013	12.0	0.6	80%	0.48	0.24
7-1-2013	15.0	3.0	80%	2.40	1.20

For the total period of the model simulation, the estimated recharge is displayed as a time series for the rural area in Figure 3.3. The average amount of net groundwater recharge for the rural area in the valley of Visp is estimated at 0.58 mm/day (average infiltration factor is 0.37). From the figure, it appears that the summers in Visp are extremely dry, yielding estimated groundwater recharge values of 0.10 mm/day. On the other hand, the winters yield significant enlarged values for groundwater recharge of more than 10 mm/day occasionally.

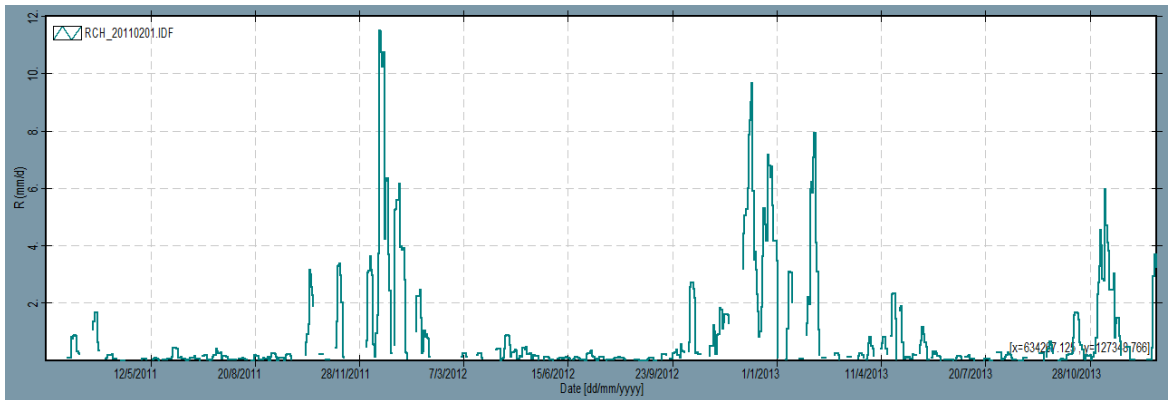


Figure 3.3 Estimated groundwater recharge (mm/day) for the rural areas.

### 3.2 Boundary Conditions

The model boundary is mainly defined by the topography. All areas above 687.5 m+MSL are excluded from the model, as this is roughly the altitude at which bedrock outcrops. For the Vispental, lower elevation was used (655.0 m+MSL) to exclude the outcrop of rocks on the east of the narrow entrance of the valley. There are three types of boundary conditions in the model, see Figure 3.4:

- 1 *Fixed potential boundaries* that let groundwater flow in and out the model to/from the outer region;
- 2 *Closed model boundaries* that don't allow any exchange of groundwater in and out the model. Note: The input from Baltschiederteral (steep alpine valley to the North) has not been taken into account at this stage;
- 3 *Fixed flux boundaries* that simulate an inflow from the mountains or from the bedrock to the Quaternary deposits (i.e. geothermal groundwater circulation).

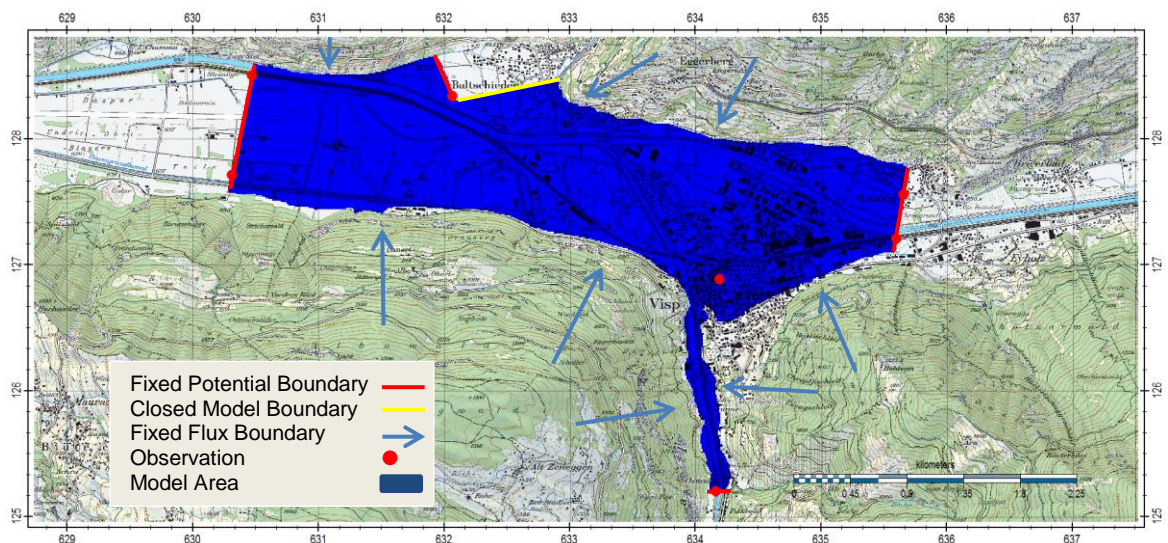


Figure 3.4 Model area and the layout of the chosen model boundaries.

The different type of boundary conditions will be explained in more detail in the following subsections.



### 3.2.1 Fixed Potential Boundary

The fixed potential boundaries allow groundwater to flow in or outside the model domain. The concept of these boundaries is a fixed groundwater heads that act as source or sinks to keep the groundwater head at the prescribed level. This type of model boundary assumes that any measure in the model domain does not influence the fixed groundwater head on the model boundary. For example, whenever a groundwater extraction is planned near the boundary condition, it probably influences the groundwater level on the boundary as well and therefore the chosen location for the model boundary is not valid anymore. The *characteristic length* is a measure of the spatial effect of hydrological interventions. The *characteristic lengths*  $l$  has the following general mathematical formulation  $l = \sqrt{\Sigma T \Sigma C}$ , where  $\Sigma T$  is the total transmissivity (assumed to be 2000 m<sup>2</sup>/day) and  $\Sigma C$  (500 days) the total vertical resistivity. In the Visp the *characteristics length*  $l$  comes to 150 meter. Measures within 450 meter ( $3 \times l$ ) of the open model boundaries should therefore not be included. Several observation wells are selected to represent the fixed potential boundaries, see Figure 3.5.

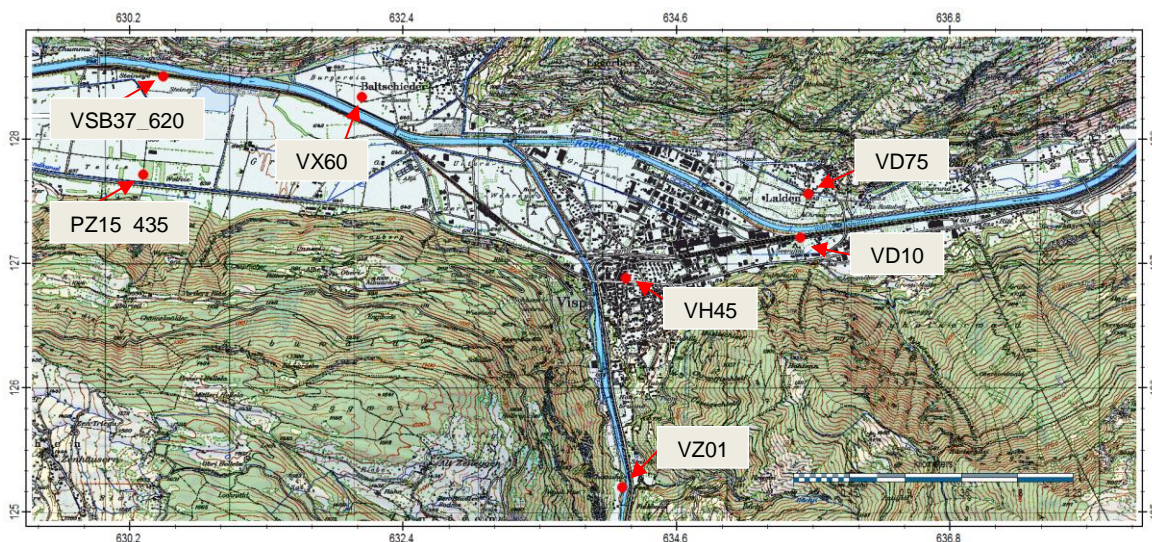


Figure 3.5 Locations for the selected observation wells for the boundary conditions.

#### Western boundary in Rhône:al:

The model boundary on the west is formed by the observation wells PZ15\_435 (mean level is 635.92 m+MSL) and VSB37\_620 (mean level is 636.53 m+MSL) which are both measured on a daily base, see Figure 3.7. The amplitude of VSB37\_620 is approximately 3.5 meter due to the water level in the Rhône, as the amplitude of PZ15\_435 is significantly less: 0.6 meter. The difference between the mean values for the two observation wells is 0.6 meter and they are 800 meter next to each other. In between the groundwater level changes significantly. Therefore, the fixed groundwater levels along the western open model are declining from the north (VSB37\_620) to the south (PZ15\_435). Missing data in between both measurements have been filled up by linear-regression, whereby  $VSB37\_620 = 0.22 \times PZ15\_435 + 495.7$  (regression coefficient  $R^2=0.79$ ), see Figure 3.6-left.

#### Eastern boundary in Rhône:al:

The differences for VD75 and VD10 are smaller. Their mean values are 645.85 m+MSL (VD75) and 646.30 m+MSL (VD10) and have similar dynamics (4.0 meter), as their distance is 370 meter. The fixed groundwater levels along the eastern boundary are nevertheless equally processed as for the western boundary, though VD75 misses observation for the period 16<sup>th</sup> of November 2012 up to the 21<sup>st</sup> of February 2013. For these periods the

measured regime for VD10 has been used to fill in the missing data by:  $VD10 = 1.02 \times VD75 - 9.87$  (regression coefficient  $R^2=0.97$ ), see Figure 3.6-middle.

#### *Southern boundary in Vispताल:*

The groundwater level further up in the Vispताल (VZ01) has been measured daily since the 7<sup>th</sup> of August 2013. For the period before that, the groundwater level has been estimated by the relation of this observation well VZ01 and the nearest observation well VH45. The mean values for both observation wells VZ01 and VH45 are 654.22 m+MSL and 643.38 m+MSL, respectively. The absent measurements for VZ01 are determined by the linear-regression formulae  $VZ01 = 1.6 \times VH45 - 387.5$  (regression coefficient  $R^2=0.96$ ), see Figure 3.6-right.

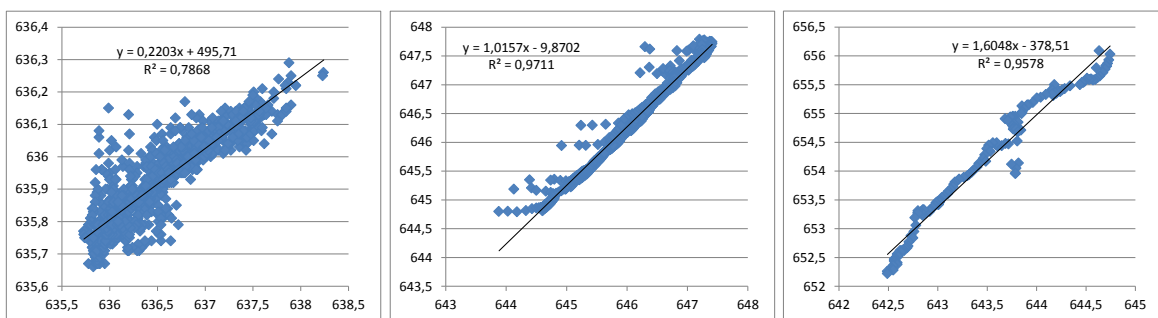


Figure 3.6 Scatter plots of the measured observations for the boundary conditions, (left) VSB37-PZ15, (middle) VD75-VD10 and (right) VH45-VZ01.

#### *Boundary in Baltschieder area:*

The area around Baltschieder is not part of the current modelling. To include the inflow from this area into the model, the observation well VX60 is used to simulate the exchange of groundwater.

All corrected observation has been depicted in Figure 3.7.

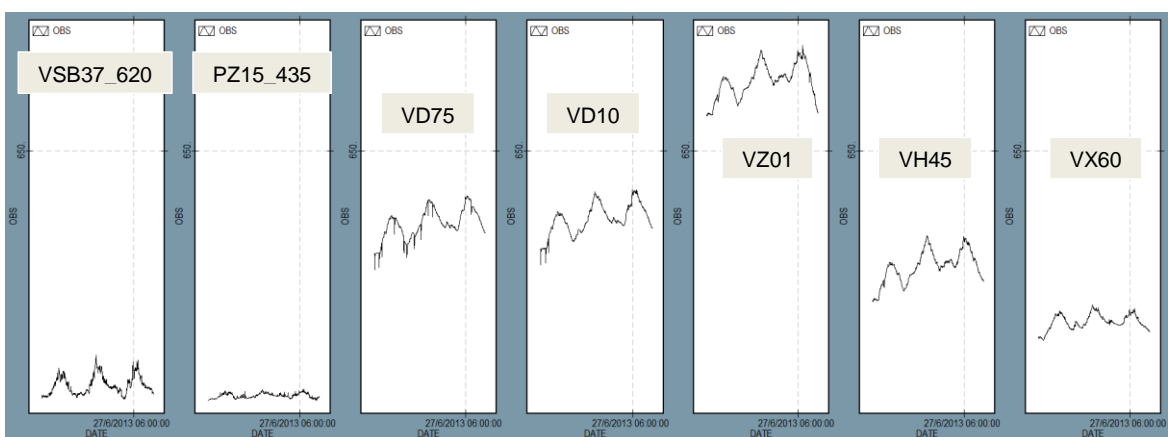


Figure 3.7 Times series for the observation wells of the fixed potential boundary conditions.

### 3.2.2 Closed Model Boundary

As mentioned before, the contribution from Baltschieder has not been taken into account in the current modelling. The main groundwater flow gradient in Baltschieder area is orientated from the East to West. To enforce this, an artificial no-flow boundary is implemented in the model perpendicular to this. The Baltschieder area itself has been blocked out in the simulation.

### 3.2.3 Fixed Flux Boundary

Precipitation and snow melt water flow from the mountain hills into the valley and determine a part of the total inflow in the aquifers of the Rhône valley. The amount of water is estimated to be equal to the net total volume in a sub catchment area as computed by the methodology as described by the *Geotechnisches Institut, June 2015*. Here, it has been found that the groundwater level (i.e. side-inflow into the aquifer) can be correlated ( $R^2=0.5$ ) with the measurements of the snow water equivalent with a moving average of 210 days. This gives more realistic inflow dynamics than if the snow water equivalents are used directly as inflow.

Each sub catchment area aligns with the slopes in the topography. In Figure 3.8 those catchment areas are delineated by different colours and numbers. The total amount of estimated ground water recharge in the sub catchments are summed up and distributed evenly along the downhill boundary of each sub catchment.

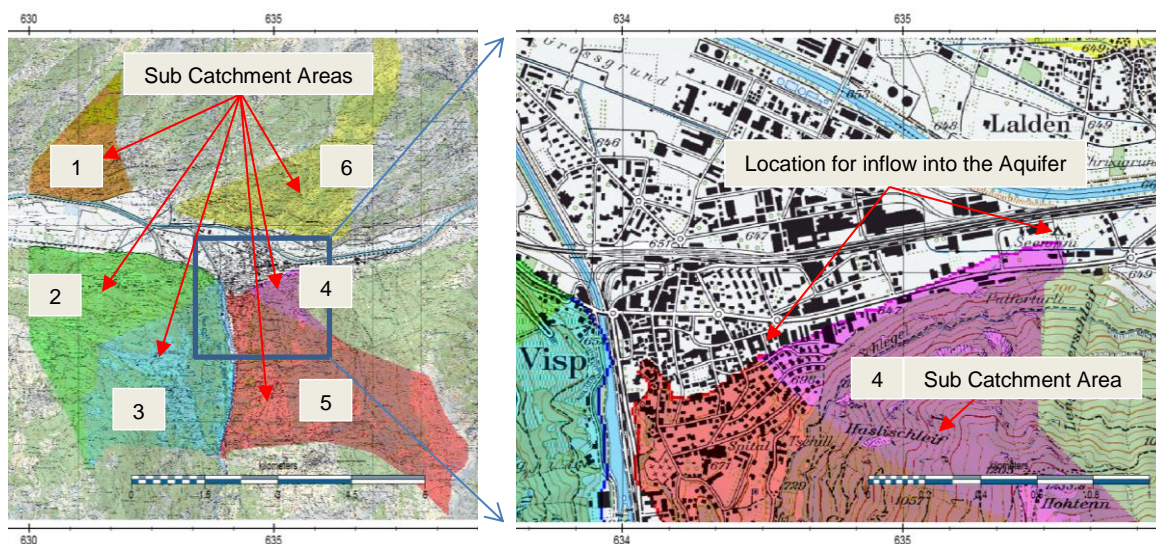


Figure 3.8 Layout of the six sub catchment areas that discharge directly into the aquifer of the Rhône valley.

Besides the time varying inflow from the mountains that enters the aquifer from the sides, a constant inflow of 0.5 mm/day is assigned at the top of the hard-rock (value defined by the Geotechnisches Institut at a meeting on 21<sup>st</sup> of May 2015 at Deltares). This takes into account groundwater entering the Rhone-Valley aquifer system from a great depth, as evidenced by a few deeper boreholes, where sub thermal groundwater ( $T>20^{\circ}\text{C}$ ) has been documented at approx. 100 m depth, confirming the presence of a hydrothermal circulation at depth and the interaction between the bedrock and the Quaternary deposit.

### 3.3 Groundwater level Observations

Nearby the village of Visp, six groundwater level observations are selected to qualify the performance of the model, see Figure 3.9. They are used to optimize some parameters in the model such that the difference between measured and modelled groundwater level is minimized within a plausible / realistic bandwidth.



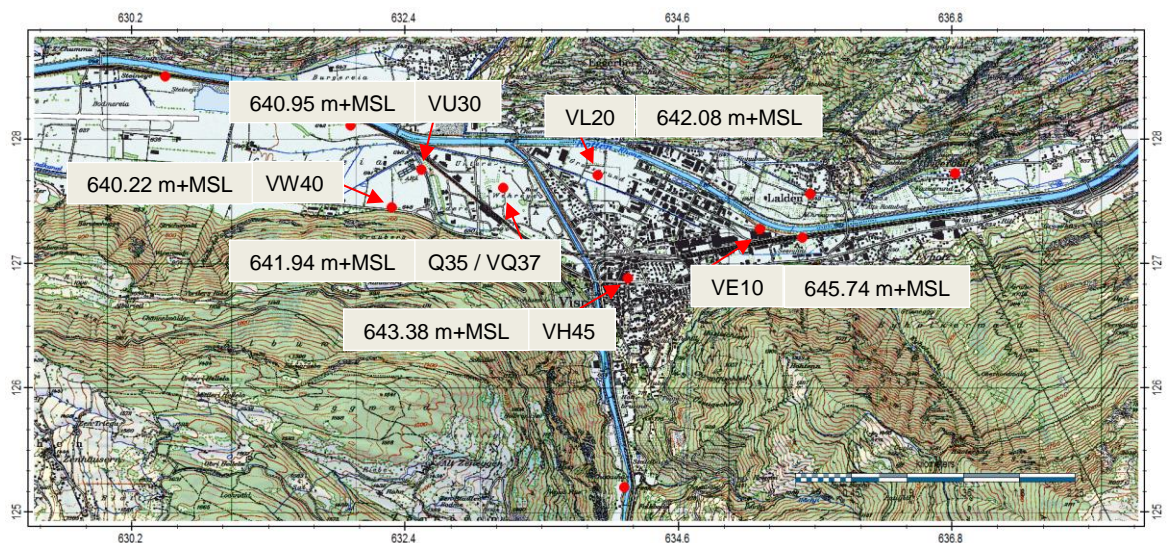


Figure 3.9 Location of the six observation wells used for quality-control of the model and the averaged values for calibration purposes.

The time series are depicted in Figure 3.10. The observations in wells Q35 and VQ37 are identical at the moment Q35 stops (1<sup>st</sup> of January 2013) and, VQ37 starts monitoring (14<sup>th</sup> of February 2013). Except for VH45, all observation wells show some non-continuity in their monitoring. Both, VW40 and VL20, show a large gap in their monitoring data for 2012. Furthermore, VE10 is very close to the fixed potential boundary and does not have a significant additional value. The most important observation wells are therefore VH45 and VU30 with continuous time-series available.

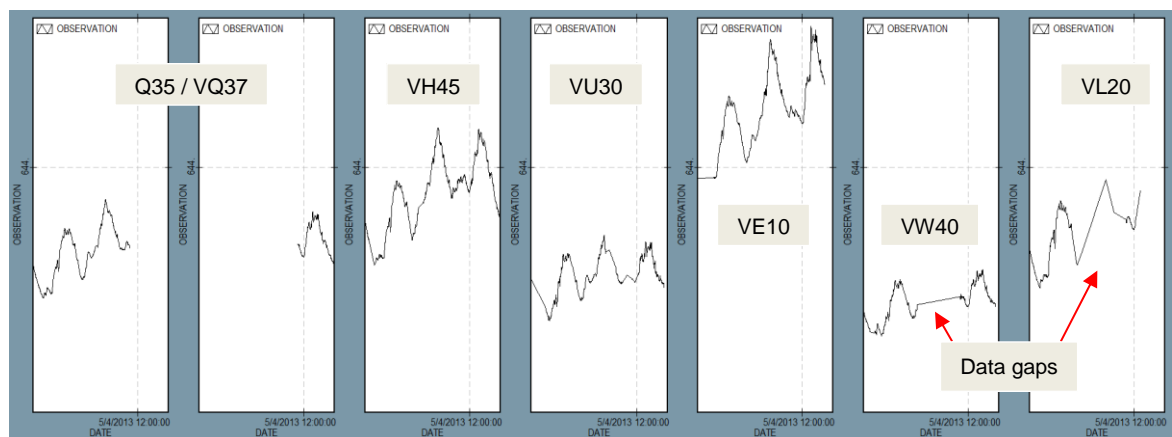


Figure 3.10 Times series for the observation wells for calibration.

All observations are compared with the computed hydraulic head for model layer 1, which represents the first (topmost) aquifer.

### 3.4 Initial Groundwater level

The averaged groundwater level is computed by the steady-state model. Because a transient simulation starting at the 1<sup>st</sup> of February 2011 would take a couple of weeks to reach equilibrium from this steady-state solution, we have used instead an interpolated groundwater level based upon the measurement for the 1<sup>st</sup> of February 2011. The interpolation was done using Ordinary Kriging (range = 3 km), see Figure 3.11, taking into account all available observation as presented in Figure 3.5 and Figure 3.9.

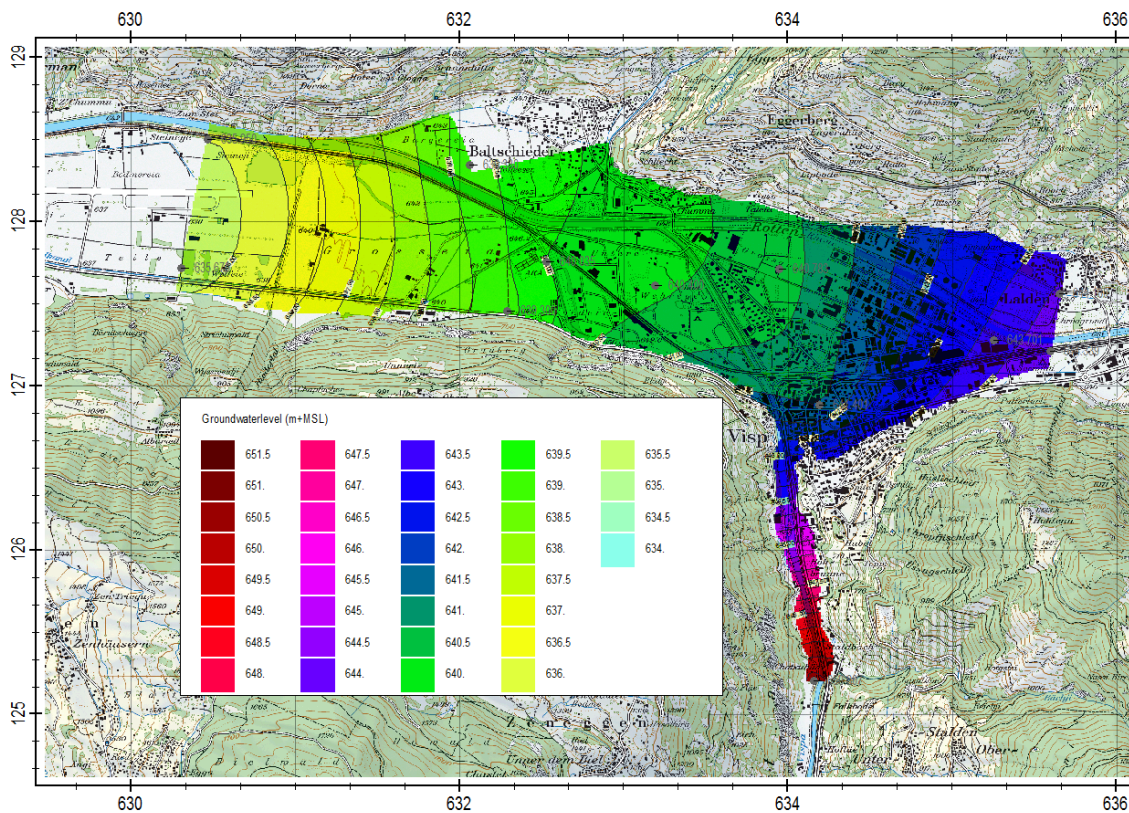


Figure 3.11 Interpolated groundwater level (Kriging) for the 1<sup>st</sup> of February 2011.

### 3.5 Surface Water

Within the model area, the most determining water ways are the rivers Rhône and Vispa, see Figure 1.1. The Rhône is flowing from the east to the west, as the Vispa flow from the south to the north and intersects with the Rhône, north of Visp. Both rivers discharge permanently, but show large fluctuations in their water levels. The amount of water that exchanges between groundwater and surface water is mainly caused by the difference between the groundwater- and surface water levels. In the following subsections the determination of the surface water levels are outlined.

#### 3.5.1 Rhône River

The nearest observation stations for the Rhône are the stations MQA and MQB at the eastern boundary of the model and station 2346 (6.5 km further upstream in Brig). This station has daily measured water levels as MQA and MQB measures water levels hourly. The latter stops monitoring since the 28<sup>th</sup> of April 2011 and has been left out. MQA has a data gap for the period in between 27<sup>th</sup> of April 2012 and 5<sup>th</sup> of May 2012 that has been filled in with measurement from Brig. From the measurements between Brig and MQA the average difference is estimated at 17.3 m, thus for the missing data, MQA has been filled in by applying  $MQA = BRIG - 17.3$ , see Figure 3.12. High peaks are occurring in the summer months (approximately 2 meter) and low levels in the winter.

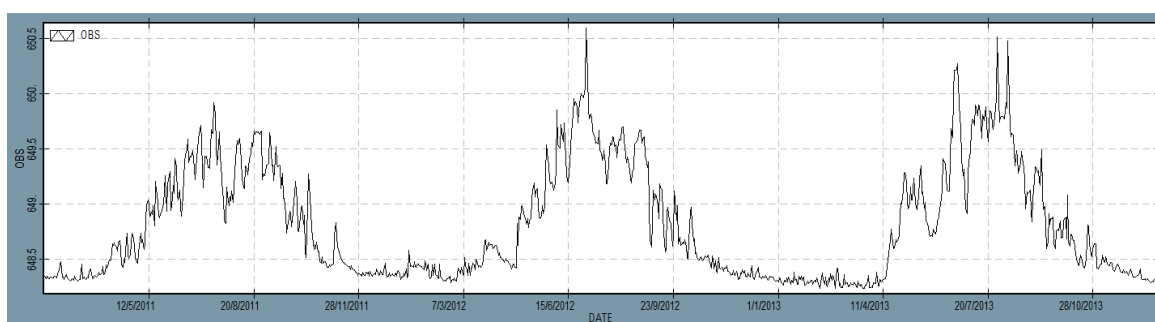


Figure 3.12 Measured water levels at MQA, filled in partly with measures from station 2346 (Brig).

From the east to the west of the model, it is assumed that the water levels in the Rhône can be interpolated linearly. On the east, MQA is located at the local distance (HEC-RAS) of 112.231 km. This corresponds with a bottom level of 648.16 m+MSL (BAFU, 2013). As the water level is minimal 648.24 m+MSL, the resulting minimal water depth is  $\approx 0.10$  m, the maximal water depth is estimated at 2.43 m, see Table 3.3.

To the west (STG near St. German), the bottom level of the Rhône is estimated at 634.93 m+MSL (HEC-RAS is 106.598 km, BAFU, 2010). The difference is 13.23 m and the water levels at the western boundary STG are therefore computed as  $STG = MQA - 13.23$  m.

It is important to determine an extra water level at the junction with the Vispa, as the gradient of the Rhône probably changes downstream the junction due to the increased discharge and channel width. Just before the junction of the Rhône and Vispa, the bottom level is estimated at 642.46 m+MSL – after the junction – the bottom level is estimated at 640.68 m+MSL.

Table 3.3 Estimated water levels in the Rhône for the model area.

Station	HEC-RAS (km)	Bottom Level (m+MSL)	Width (m)	Min Level (m+MSL)	Max Level (m+MSL)	Average Level (m+MSL)	Average Water Depth (m)
2346 Brig	118.33	665.07	36.0	665.45	667.43	665.93	0.86
MQA	112.23	648.16	36.0	648.24	650.59	648.80	0.64
Before Vispa	109.46	642.46	36.0	642.54	644.89	643.10	0.64
Vispa	109.31	640.68	50.0	640.76	643.11	641.32	0.64
St. German	106.60	634.93	50.0	635.01	637.36	635.57	0.64

The dimensions of the Rhône have been estimated by measuring the width from the topographical map.

### 3.5.2 Vispa River

The nearest measurement station 2351 for the Vispa River is within the model boundary. The station has daily measured water levels.



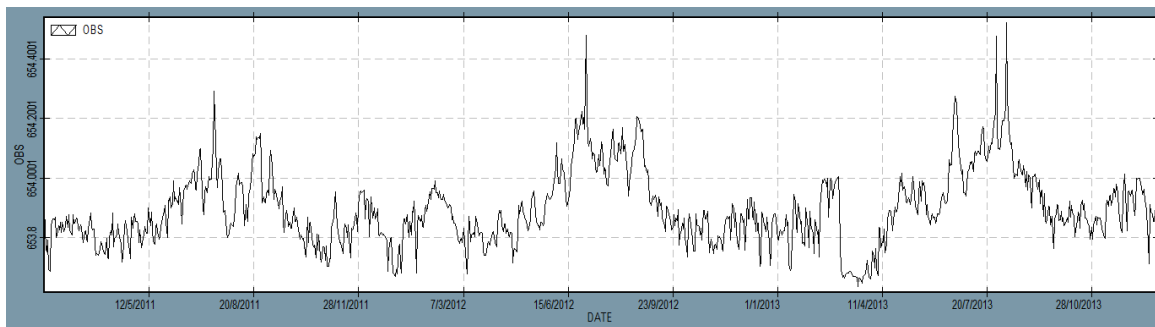


Figure 3.13 Measured water levels at station 2351.

A similar methodology has been used to determine the water levels at characteristic location along the Vispa River. The bottom level at the old station 2351 is estimated at 656.25 m+MSL (HEC-RAS 3.19 km); this station lies outside the model boundary. The station has been moved 1.0 km further downstream in 1996 and the bottom level at his renewed location is estimated at 653.36 m+MSL (HEC-RAS 2.3 km from the intersection with the Rhône River, BAFU, 2010). There is a waterfall downstream the station whereby the bottom level is estimated at 650.48 m+MSL. Near the intersection with the Rhône River, the Vispa River drops from 643.76 m+MSL to 640.68 m+MSL.

Table 3.4 Estimated water levels in the Vispa for the model area.

Station	HEC-RAS (km)	Bottom Level (m+MSL)	Width (m)	Min Level (m+MSL)	Max Level (m+MSL)	Average Level (m+MSL)	Average Water Depth (m)
Rhône	0.00	640.68	20.0	640.76	643.11	641.32	0.64
Visp Waterfall	0.10	643.76	20.0	643,84	646,19	644,4	0.54
DownS 2351	2.30	650.48	20.0	650,56	652,91	651,12	0.54
UpS 2351	2.31	653.36	20.0	653,44	655,79	654	0.54
Old Stat. 2351	3.19	656.25	20.0	656,33	658,68	656,89	0.54

The dimensions of the Vispa River have been estimated by measuring the width from the topographical map.

### 3.5.3 Rhône and Vispa Rivers

The resistance of the riverbed for the Rhône and the Vispa Rivers are initially estimated at 1.0 day. This is an initial estimate as it will be subject to the parameter optimization, such that the exchange of surface and groundwater will be in the order of 20-100 l/s/km (see WEA, 1999; AfU Solothurn, 2008; WEA, 2004). At the location of the weirs (in the Vispa and at the intersection of the Vispa and the Rhône) the resistance is 10,000 days due to concrete material that will be at the bottom near the weirs.

For each day, the water levels are interpolated linearly between the stations as defined in Table 3.3 and Table 3.4. Whenever the computed water level is presented in a three-dimensional presentation, the outline of the Rhône and Vispa River in the model area becomes clear, see Figure 3.14.

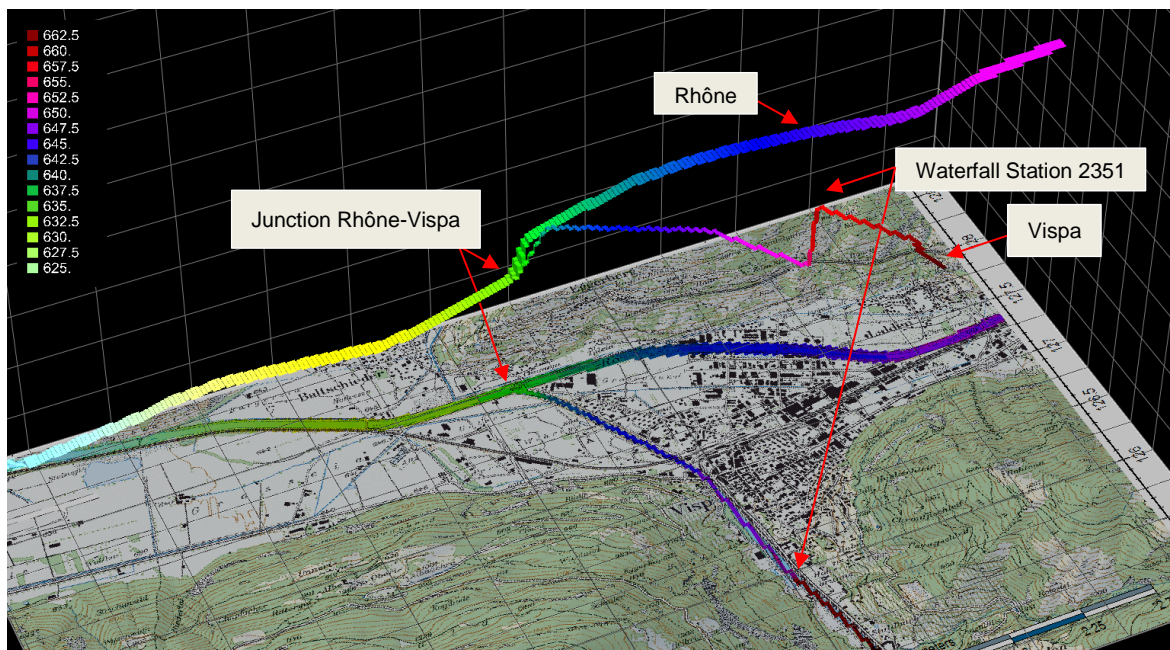


Figure 3.14 Three-dimensional representation of the computed water levels for the Rhône and Vispa River.

### 3.6 Groundwater Extractions

There are three main major categories for groundwater extraction in the area of Visp (N. B. Ground source heat pumps are not considered in the framework of this study):

- 1 Drinking water supply for the municipality of Visp;
- 2 Cooling water for the Lonza industry as a supplier for the pharmaceutical and biotechnology industries with biopharmaceuticals;
- 3 Local, private extractions for artificial recharge and other water usage.

All extractions are positioned in the second model layer that represents the uppermost aquifer, their locations (category 1 and 2) are presented in Figure 3.15 and category 3 is presented in Figure 3.16.

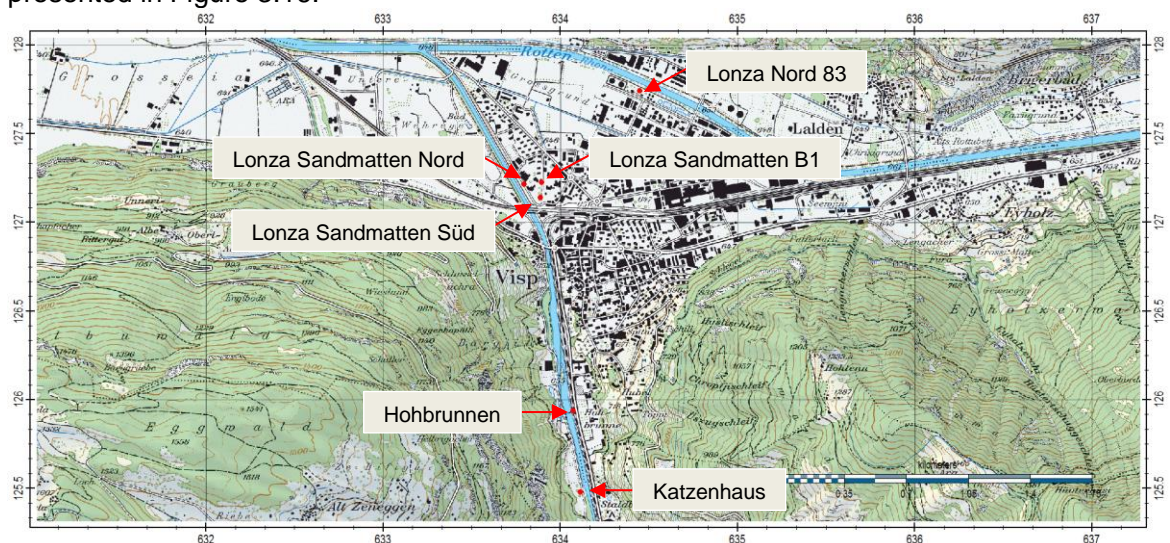


Figure 3.15 Location of extraction wells for drinking (Hohbrunnen/Katzenhaus) and industrial use (Lonza, 4 distinctive wells).



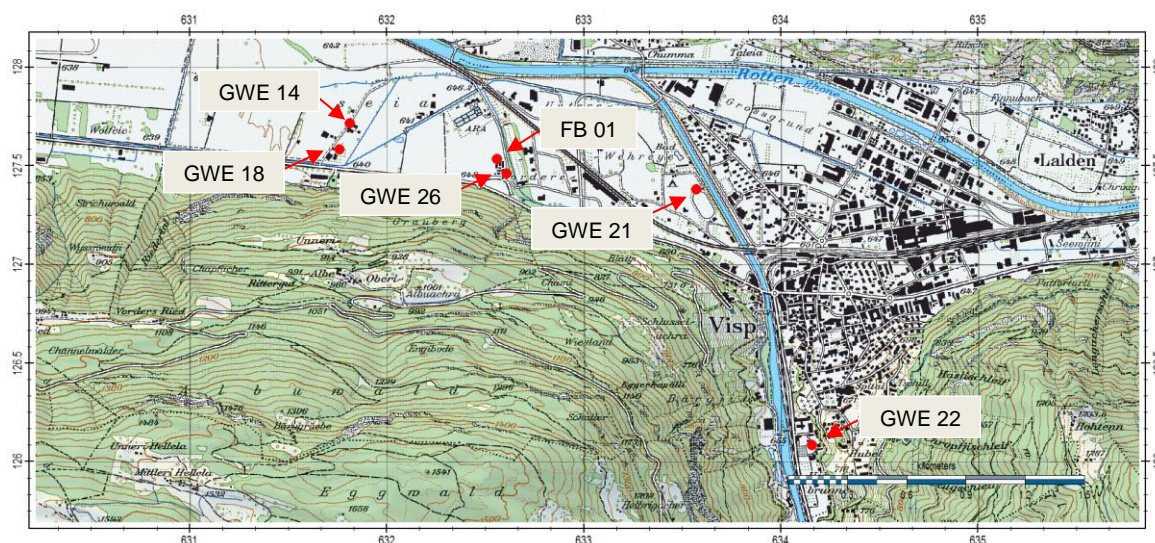


Figure 3.16 Location of selected extraction wells for artificial recharge and other usages.

The available extractions are listed in Table 3.5 and are divided into the three categories: industry (red), drinking water (blue) and agricultural purposes (green). The extractions for the industry and drinking water are given by daily and monthly rates respectively, see Figure 3.17 and Figure 3.18. For the agriculture (green category), the mentioned values are the licensed rates rather than the effective rates. For the model, the effective rates are assumed to be 50% of the licensed rates (column with maximal values in Table 3.5) and applied only during the months May, June and July of each year. For the total averaged rate (used by the steady-state model), the effective rate is equal to  $0.5 \times 0.25$  of the licensed rates.

Table 3.5 Existing extraction locations and corresponding rates nearby Visp for different categories.

Station	X	Y	Q (m <sup>3</sup> /day) Licensed	Q (m <sup>3</sup> /day) Average	Q (m <sup>3</sup> /day) Minimal	Q (m <sup>3</sup> /day) Maximal
Lonza Nord 83	634449	127744		6887.0	0.0	9550.0
Lonza Sandmatten Nord	633794	127217		218.0	0.0	3550.0
Lonza Sandmatten Süd	633888	127142		2389.0	0.0	5400.0
Lonza Sandmatten B1	633893	127226		5152.0	0.0	9550.0
Hohbrunnen (24m-surf.lvl)	634071	125937		644.0	0.0	2100.0
Katzenhaus (30m-surf-lvl)	634113	125480		1134.0	0.0	3750.0
GWE 14 F.Häfliger*	631812	127715	2016.0	198.0	0.0	1008.0
GWE 18 M.Stalder <sup>#</sup>	631761	127583	2016.0	198.0	0.0	1008.0
GWE 21 Sportplatz*	633569	127380	1152.0	144.0	0.0	576.0
GWE 22 Landwirsch. S.*	634156	126083	1728.0	144.0	0.0	864.0
GWE 26 Diverse Bauern*	632609	127461	864.0	108.0	0.0	432.0
FB 01 DUS <sup>#</sup>	632558	127536	288.0	36.0	0.0	144.0
Total				17252.0	0.0	37932.0

<sup>#</sup>other water usage; \*artificial recharge

The maximal total amount of groundwater extracted is estimated at 37'932 m<sup>3</sup>/day, the minimal amount is set for the case where no artificial recharge occurs and both industrial and drinking water are inactive, namely at 0.0 m<sup>3</sup>/day. Of course, these values over- and underestimate the reality since the effective extraction per day is the result of a variable combination between the different extractions listed in Table 3.5. In Figure 3.17 the extraction

rates are presented for the Lonza industry. The extractions at the different well locations vary significantly.

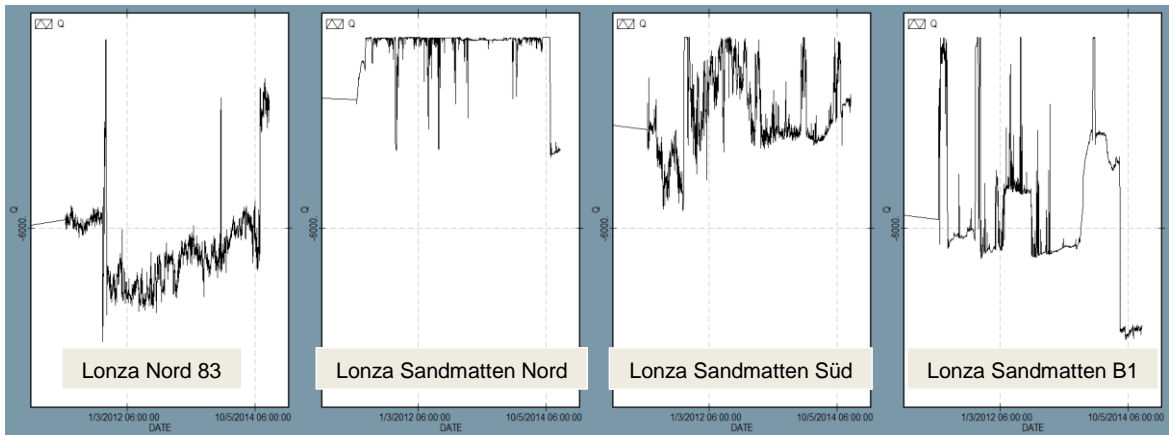


Figure 3.17 Measured extraction rate in  $\text{m}^3/\text{day}$  for the Lonza Industry between 2010 and 2014.

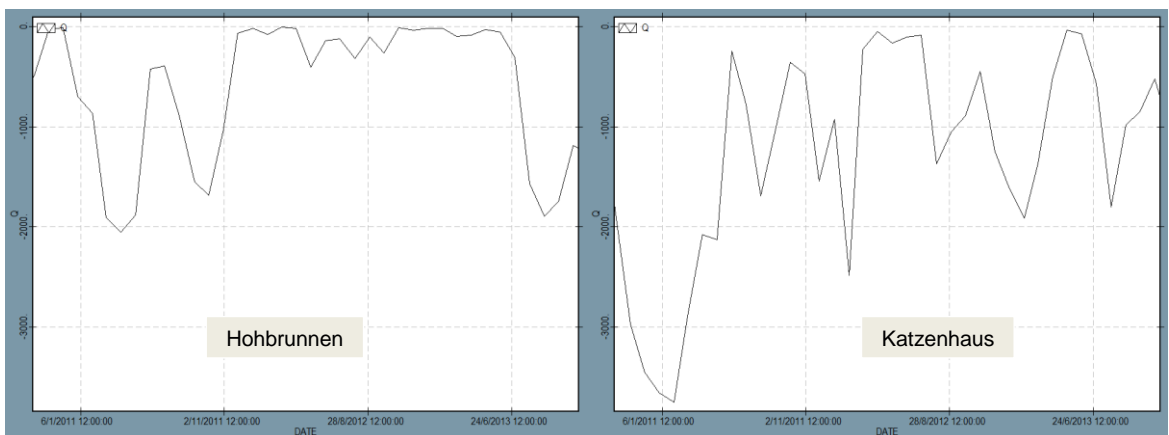


Figure 3.18 Measured extraction rate in  $\text{m}^3/\text{day}$  for the Drinking water supply for the municipality of Visp between 2011 and 2013.

### 3.7 Cellars

Within the city of Visp, several underground infrastructures (cellars, parking lot, piles, e.g. “elements”) are built in the subsoil. As visible on Figure 3.19, these have been subdivided into shallow elements (average 3 m below surface level), deep elements (6 m below surface level) and very deep elements (12 m below surface level)..

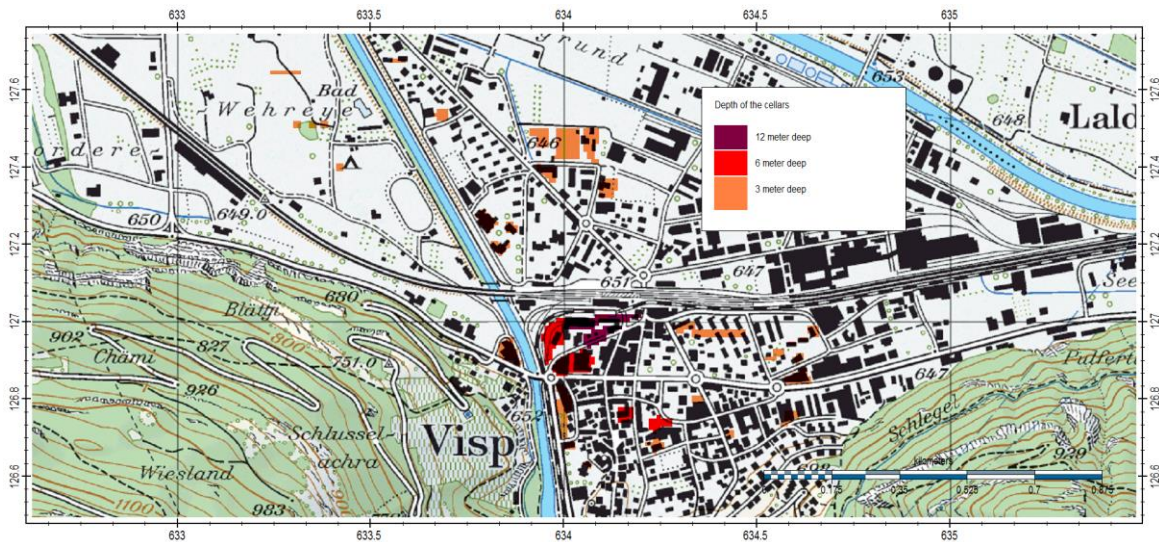


Figure 3.19 Overview of the major underground infrastructures ("elements") in the city of Visp, coloured by their estimated depth in meter below surface level (source: Municipality of Visp)

Those elements have an obstructing effect for groundwater flow, especially whenever they are penetrating in water bearing layers, such as the fluvial deposits. Within the model, the geology has been adjusted for the location of the elements – in fact the existing soil has been removed and the thickness of the water bearing – or low permeable layer has been reduced according the depth of penetration, see Figure 3.20.

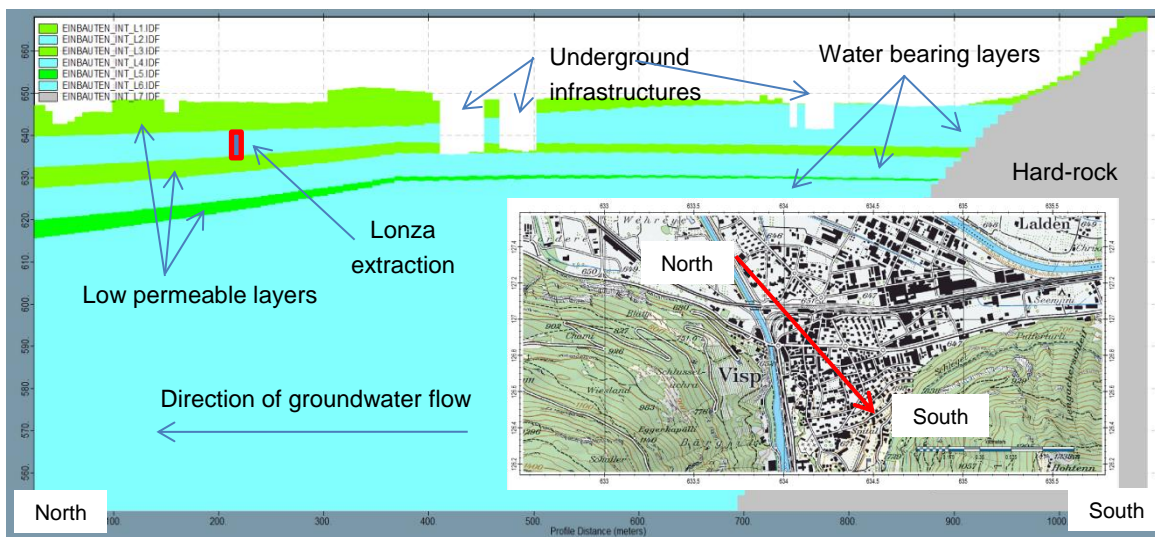


Figure 3.20 Cross-section showing the penetration of the elements depicted in Figure 3.19.



## 4 Optimization

### 4.1 Introduction

Automatic parameter optimization is an “art” as there is always the danger of over-fitting the model to the parameters. It should be realized that – in theory – a parameter set could be found that minimizes the misfit (penalty function) between the measurements and the computed values to a value of zero. The penalty function is the sum of the quadratic difference between the measurements and the computed values. As a result, the selected parameters often need to be adjusted far beyond their reliability. In those cases the model will be fitted to the measurements, meaning abuse of automatic optimization. The art of optimization is on the contrary to select the appropriate parameters and to stop on time, just before the process of fitting starts.

Parameters that can be optimized in the model need to be sensitive. This means that a slight modification of the parameter yields a (significant) improvement or deterioration of the misfit. Parameters that are less sensitive need to be adjusted significantly to alter the misfit and therefore it could be stated that they are “abused” to minimize the misfit. Moreover, any misfit of the model needs to be corrected by the chosen set of parameters. The more parameters, the more the misfit will be reduced and the less drastic individual parameters need to be adjusted. It is never possible to have more parameters optimized, than the number of observations. In this model, the number of unique locations with observations is 6 – however 4557 individual observations are available during the model simulation period. This makes it more feasible to select more than 6 parameters during the optimization, though with care, since within the 4557 observation, there may be a large redundancy of information.

In this study, the transient model has been optimized for four different sets of parameters. To increase the performance of the optimization, the model has been simulated on a 50 x 50 m resolution.

#### 4.1.1 Optimization with parameter set 1

The first set of parameters that has been optimized is the Leakage Factor LF of the Vispa and Rhône, the porosity P and the specific storage coefficient SS. The results are presented in Table 4.1.

Table 4.1 Optimization results for the first set of three parameters

		Initial value	Correlation Coefficient C			Optimized value
			LF	P	SS	
<b>LF</b>	Leakage Factor (d)	1.0	1.00	0.26	-0.15	0.1
<b>P</b>	Porosity (-)	0.120		1.00	-0.97	0.21
<b>SS</b>	Specific Storage (-)	3.5E <sup>-4</sup>			1.00	8.40E <sup>-6</sup>
	Sensitivity (%)		68.5	29.8	1.7	
	Penalty function (m <sup>2</sup> )	6714				2320

The leakage factor is reduced to 0.1, which means that the infiltration capacity of both rivers becomes 10 times lower. The porosity P and specific storage coefficient SS are highly correlated (C = -0.97) which means that they tend to vary dependently in the opposite direction to minimize the penalty function. Parameters that are highly correlated are difficult to estimate simultaneously, though the condition number N (ratio of the highest to lowest



eigenvalue of the parameter error covariance matrix) is rather low (17). According to Doherty (2015), as long as the condition number  $N$  is less than  $5 \times 10^7$ , the numerical integrity is non-questionable.

Since, the specific storage coefficient  $SS$  is less sensitive than the specific porosity  $P$ , it has been adjusted more. The computed versus the measured groundwater heads for VH45 are presented in Figure 4.1b, but they show a poor fit; though a significant improvement compared with the original results before the optimization, see Figure 4.1a. The model is not able to predict the behaviour of the groundwater head realistic by adjusting these parameters solely, although it reduces the penalty function from 6714 down to 2320  $m^2$ .

#### 4.1.2 Optimization with parameter set 2

In the next set of parameters the permeability of the Vispताल  $KV$  has been included. The results of the optimization are given in Table 4.2.

Table 4.2 Optimization results for the second set of four parameters

		Initial value	Correlation Coefficient C				Optimized value
			KV	LF	P	SS	
<b>KV</b>	Vispताल (m/d)	50.0	1.00	-0.91	-0.16	0.07	45.0
<b>LF</b>	Leakage Factor (d)	1.0		1.00	0.26	-0.13	0.1
<b>P</b>	Porosity (-)	0.12			1.00	-0.97	0.22
<b>SS</b>	Specific Storage (-)	$3.5E^{-4}$				1.00	$1.3E^{-6}$
	Sensitivity (%)		27.7	48.3	23.8	0.2	
	Penalty function ( $m^2$ )	6714					2260

The penalty function is reduced a bit more by optimizing the set of parameters, down to 2260  $m^2$ . The permeability of the Vispताल  $KV$  is reduced to 45.0 m/d, but may have been reduced even more by the optimization procedure if this was not sustained. The permeability in the Vispताल  $KV$  is negatively correlated ( $C = -0.91$ ) with the leakage factor  $LF$  which is logical. The effects of a lower inflow from the Vispताल (low permeability) could be compensated at the same order of magnitude by higher inflow from the rivers. Again the porosity  $P$  and specific storage coefficient  $SS$  are highly correlated. The measured and computed groundwater heads for VH45 are still showing a significant misfit, see Figure 4.1c.

#### 4.1.3 Optimization with parameter set 3

To improve the fit of the behaviour of the groundwater level; the permeability values within the Rhone valley  $KF$  are included. These are permeability values for the fluvial deposits (model layers 2 and 4 simultaneously). The results of this set of parameters are given in Table 4.3.

Table 4.3 Optimization results for the third set of five parameters

		Initial value	Correlation Coefficient C					Opt. value
			KF	KV	LF	P	SS	
<b>KF</b>	Fluvial Deposits Rhône valley (m/d)	125.0	1.00	0.32	0.45	-0.02	0.15	432.0
<b>KV</b>	Vispताल (m/d)	50.0		1.00	-0.62	-0.16	0.11	45.0
<b>LF</b>	Leakage Factor	1.0			1.00	0.22	-0.03	0.1
<b>P</b>	Porosity	0.12				1.00	-0.96	0.04
<b>SS</b>	Specific Storage	$3.5E^{-4}$					1.00	$9.8E^{-6}$
	Sensitivity (%)		28.4	24.5	41.2	5.1	0.8	

Penalty function (m <sup>2</sup> )	6714	902
------------------------------------	------	-----

With these five parameters, the penalty function reduces to 902 m<sup>2</sup> and the groundwater level behaves more or less similar to the observed groundwater level for VH45, see Figure 4.1d. The highest correlation is still between the porosity P and specific storage coefficient SS (C = -0.96). The most sensitive parameters are the permeability values for the fluvial deposits in the Rhône valley.

#### 4.1.4 Optimization with parameter set 4

Finally, two extra parameters are added to the optimization, those are the inflow from the sides of the valley SF (see section 3.2.3) and the inflow from the bottom of the valley BF (0.5 mm/d). The results are presented in Table 4.4 and show an additional reduction of the penalty function.

Table 4.4 Optimization results for the fourth set of seven parameters

		Initial value	Correlation Coefficient C							Opt. value
			KF	KV	LF	SF	BF	P	SS	
KF	Fluvial Deposits Rhône valley (m/d)	125.0	1.00	0.25	0.34	0.06	0.09	-0.05	0.24	432.0
KV	Vispental (m/d)	50.0		1.00	-0.62	-0.10	0.09	-0.17	0.12	45.0
LF	Leakage Factor (d)	1.0			1.00	0.15	-0.15	0.23	-0.05	0.2
SF	Sideflow (-)	1.0				1.00	-0.97	0.09	-0.03	0.3
BF	Bottom Flow (mm/d)	0.5					1.00	-0.10	0.08	1.3
P	Porosity (-)	0.12						1.00	-0.95	0.05
SS	Specific Storage (-)	3.5E <sup>-4</sup>							1.00	6.2E <sup>-5</sup>
	Sensitivity (%)		18.3	10.9	29.2	13.5	25.3	2.5	0.3	
	Penalty function (m <sup>2</sup> )	6714								894

The extra parameters for inflow SF and BF are highly correlated (C = -0.97) and even so the porosity and storage coefficient SS (C = -0.95). The computed and measured groundwater levels for VH45 are presented in Figure 4.1e.

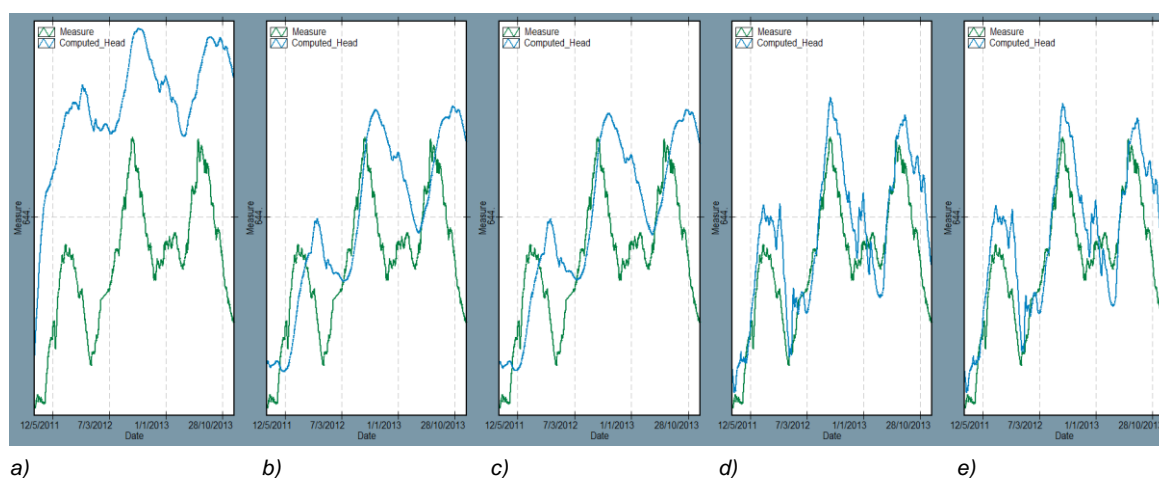


Figure 4.1 Computed versus measured groundwater levels for VH45 in Visp: a) the original results prior to the optimization; b) three parameters; c) four parameters; d) five parameters and e) seven parameters

From the optimisation it can be concluded that the permeability and storage coefficient in the Rhône valley are very important for VH45 (compare Figure 4.1c and Figure 4.1d). The

porosity of the swampy deposits (model layer 1) could indeed be low in reality, due to the poorly sorted character of the material. The reason that the porosity is increased initially in Figure 4.1b and Figure 4.1c is that this parameter is the only parameter in these parameter set configurations to lower/damp the groundwater level and reduce the misfit. The parameter is obviously used for the wrong reasons to improve the fit. The porosity  $P$  decreases to lower values whenever the permeability in the Rhône valley KF is optimized as well. The side flow SF and bottom flow BF are sensitive as well but highly correlated. The lowering of the estimated side flow improved the model even more; though this is a very difficult parameter to measure and validate in the field. For the optimization the condition number  $N=56$  and the numerical integrity is therefore acceptable.

The computed versus the observations for all locations are presented in Figure 4.2 and they all are showing an acceptable and comparable behaviour.

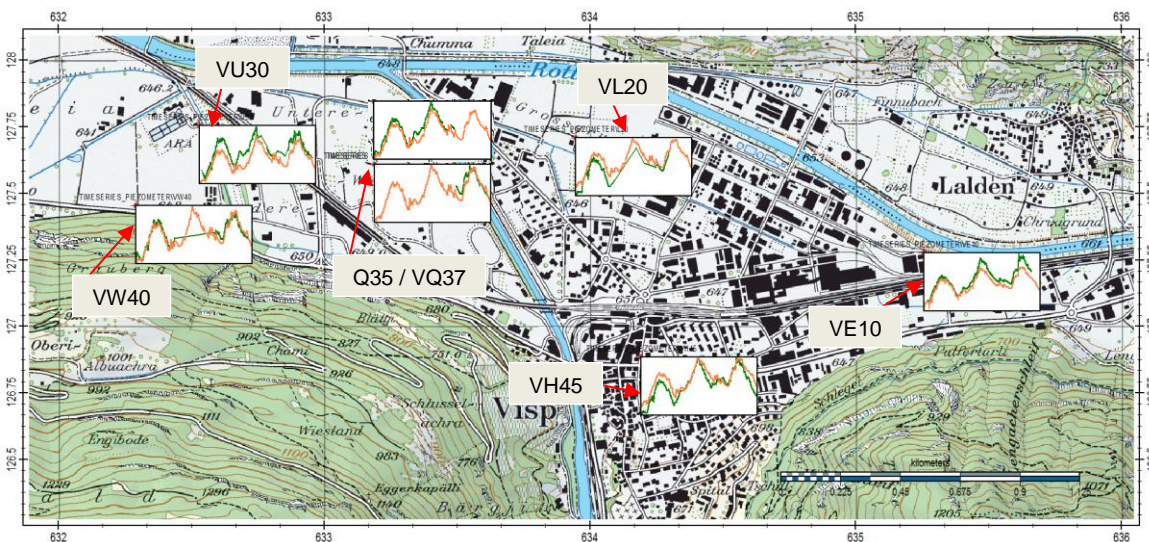


Figure 4.2 Computed (orange) and measured (green) groundwater levels for all observation wells.

To be complete, the statistics of the residuals before and after the optimization are presented in Figure 4.3. This figure shows that the histogram of the residuals is better distributed around 0 due the optimization. Besides, the histogram has become narrower. The average residual before the optimization was 0.86 with a standard deviation of 0.90 meter. After the optimization the averaged residual remains -0.03 m as the standard deviation is 0.44 m. More important are the p25 and p75 that denote that 50% of all residuals are within a difference of -0.37 m and 0.26 m. The minimal and maximal residuals are -1.25 m and 1.58 m respectively.

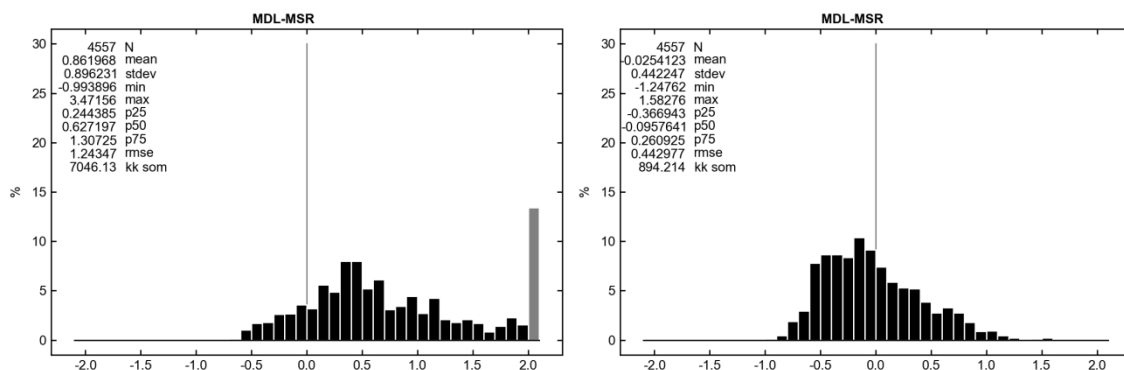


Figure 4.3 Computed statistics (left) before the parameter optimization and (right) thereafter.

Finally, it should be noticed that parameters can vary (so called parameter variance) without influencing the penalty function significantly. In other words, each parameter has a confidence interval for which the penalty function is not affected too much; these are given in Table 4.5. The minimal and maximal intervals are based upon twice the parameter variance to represent 96% of the variance of the parameter. For example, the permeability of the fluvial deposits in the Rhône valley could be varying between 382 and 487 m/d without affecting the penalty function too much. The bandwidth of uncertainty is small for porosity (0.04 - 0.07) as it is larger for the side flow SF (0.18 – 1.1). Moreover, all presented bandwidths are limited and can be used in future to evaluate the effects of uncertainty on computed scenarios.

Table 4.5 Computed parameter confidence intervals (96%). Parameter abbreviations as used in Table 4.1 to 4.4

Parameter	Min.	Average	Max.	Parameter	Min.	Average	Max.
KF	382.0	432.0	487.0	SF	0.181	0.300	1.122
KV	25.0	45.0	60.0	BF	0.073	1.300	15.321
LF	0.18	0.2	0.22	P	0.040	0.050	0.070
				SS	4.32E <sup>-6</sup>	6.2E <sup>-5</sup>	6.23E <sup>-4</sup>

## 4.2 Model Results

### 4.2.1 Groundwater levels

The transient model simulates the groundwater level fluctuation for the period 2011-2013. Here, we present the results for three characteristic periods (see also Figure 4.1), 1<sup>st</sup> of January 2012 (dry), 3<sup>rd</sup> of July 2012 (wet) and 1<sup>st</sup> of January 2013 (dry), see Figure 4.4 and Figure 4.5.



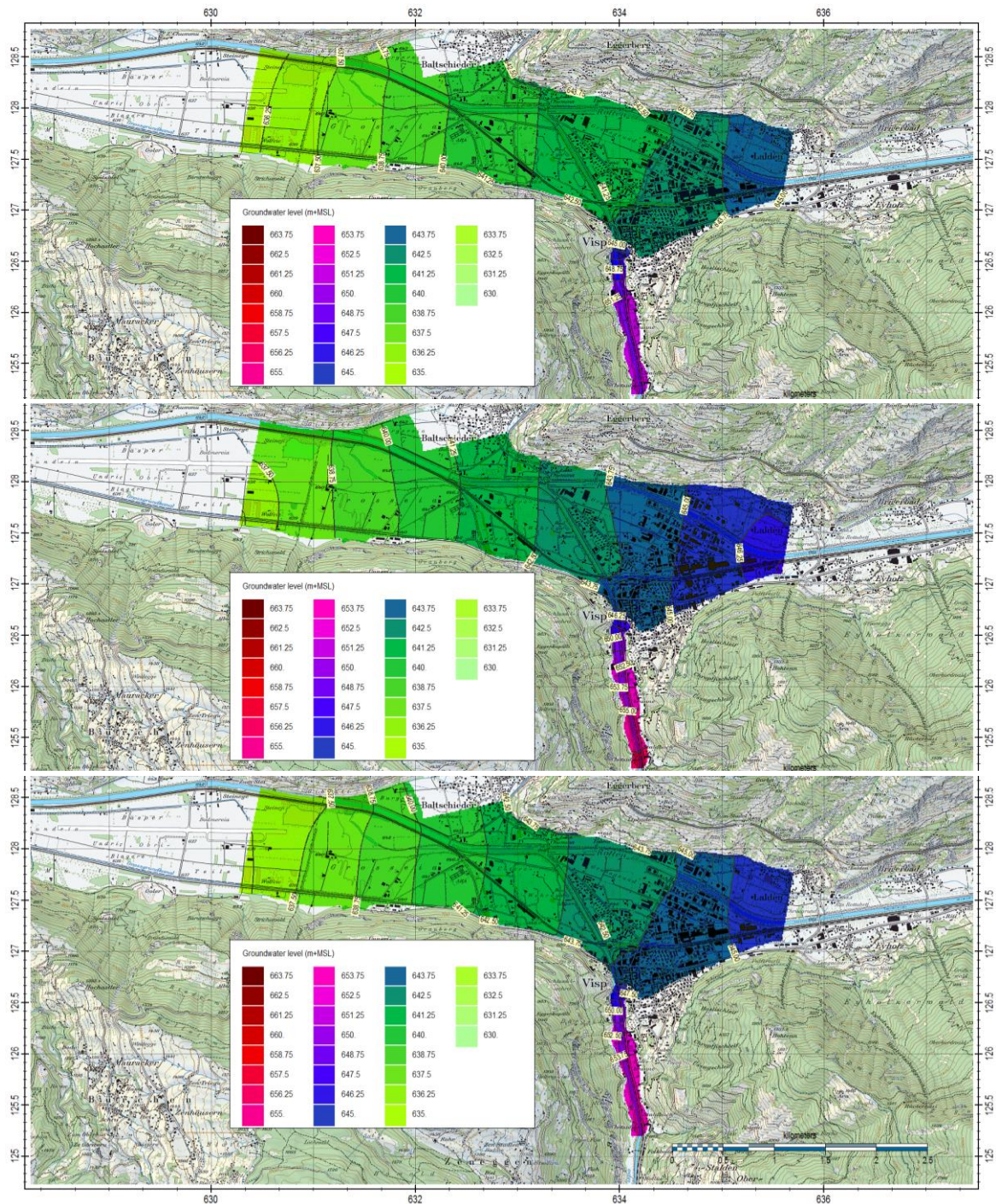


Figure 4.4 Computed groundwater level in the first aquifer (model layer 2) for top) 1<sup>st</sup> of January 2012, middle) 3<sup>rd</sup> of July 2012 and bottom) 1<sup>st</sup> of January 2013.



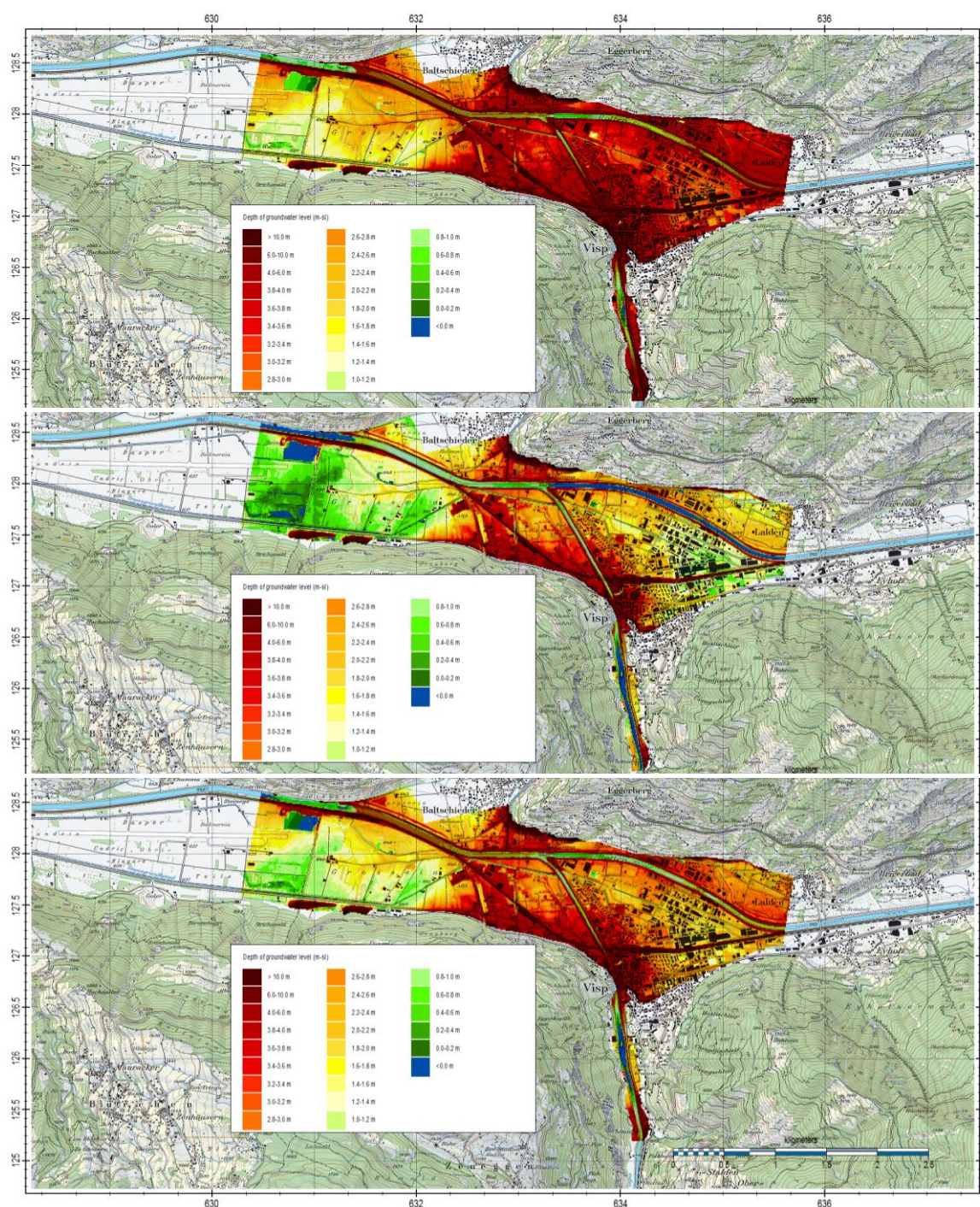


Figure 4.5 Computed depth of the groundwater table (model layer 1) for top) 1<sup>st</sup> of January 2012, middle) 3<sup>rd</sup> of July 2012 and bottom) 1<sup>st</sup> of January 2013.



#### 4.2.2 Water balance of the entire model

For three periods, the entire water balance has been constructed; 1<sup>st</sup> of January 2012 (dry), 3<sup>rd</sup> of July 2012 (wet) and 1<sup>st</sup> of January 2013 (dry). For each, the inflow components are separated from the outflow components. The different components are presented in Figure 4.6 and the corresponding water balance is presented in Table 4.6.

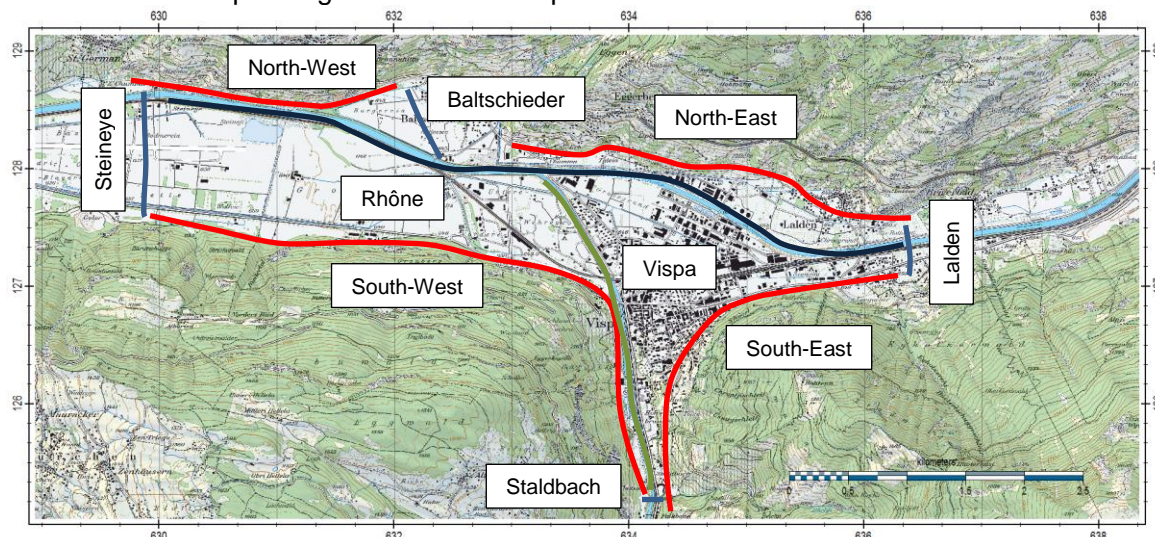


Figure 4.6 Definition of the water balance items. See also Figure 3.4 for the definition of the chosen model boundaries.

Table 4.6 Computed water balance for the entire model area.

Inflow l/s		1-1-2012	3-7-2012	1-1-2013
Fixed Potential Boundary	Vispental bei Staldbach	3.61	4.59	4.84
	Rhône bei Lalden	103.62	63.03	112.08
	Baltschieder	93.67	137.13	99.00
Infiltration Rivers	Vispa	35.71	50.19	38.11
	Rhône	45.73	128.20	30.31
Side Recharge from Mountains	North-East	3.52	8.12	5.01
	North-West	9.43	25.39	14.62
	South-West	15.60	40.34	23.64
	South-East	7.22	18.04	10.73
Areal Recharge	Groundwater recharge	326.40	11.22	215.18
	Recharge from the deep	89.27	89.27	89.27
Storage in subsoil		12.74	74.37	61.13
<b>Total Inflow</b>		<b>746.98</b>	<b>650.33</b>	<b>704.38</b>

Outflow l/s		1-1-2012	3-7-2012	1-1-2013
Fixed Potential Boundary	Rhône bei Steineye	314.78	267.42	318.32
Drainage Rivers	Vispa	0.00	7.78	4.48
	Rhône	114.76	67.81	182.35
Groundwater Extractions	Lonza Industry	195.37	162.77	179.47
	Drinkingwater Municipality of Visp	10.93	2.37	18.97
	Remaining Extraction (agriculture)	0.00	46.67	0.00
Storage in subsoil		110.51	95.38	0.70
<b>Total Outflow</b>		<b>746.35</b>	<b>650.19</b>	<b>704.29</b>

In the model domain, the Vispa has a length of 3 km; the Rhône has a length of 6 km. The infiltration capacity of the Vispa River is approximately 15.0 l/s/km on average of the complete length of the Vispa in the model. Higher infiltration capacities even occur along individual segments. The Vispa drains groundwater for a limited amount of 7.78 l/s in wet periods in the summer. The Rhône River shows an infiltration and drainage capacity of 20-30 l/s/km during the wet seasons.



## 5 Scenarios

### 5.1 Initial scenarios

#### 5.1.1 Introduction

The following scenarios have been defined:

- 1 This scenario computes the effects of the high water levels in 2012, therefore the water levels from 2<sup>nd</sup> February 2011 up to the 31<sup>st</sup> of December 2011 were applied for the similar period in 2012 and applied for:
  - a) the Vispa River only;
  - b) the Vispa River and the Rhône River;
- 2 This scenario computes the effects of the underground infrastructures in the city of Visp, see section 3.7 on page 29;
- 3 This scenario computes the effect of reducing the total extraction amounts for the Lonza industry:
  - a) reduced the total extraction rate completely;
  - b) reduced the total extraction rate for 50%.

All above mentioned scenarios have been computed for the entire model simulation period 1<sup>st</sup> of February 2011 up to the 31<sup>st</sup> of December 2013. The groundwater head in model layer 2 (first high permeable fluvial deposits) is compared with the reference situation as described in the previous sections. The results are presented as the total drawdown spatially (Appendix A) and the effect on the observation location VH45 in Visp described in the following section.

#### 5.1.2 Results

The computed groundwater head in the permeable fluvial deposits is presented in Figure 5.1 for all scenarios simultaneously. The effect of underground infrastructures in Visp has a small effect on VH45 (Scen 2). The maximal effect near the different elements is approximately 0.20 meter locally, though it has a constant effect of 0.05 meter on VH45. The adjusted water level for the Vispa River (Scen 1a) is in the same order of magnitude, i.e. maximal 0.05 meter in the time series of VH45 and only in the summer of 2012. Combined with the adjusted water levels for the Rhône (Scen 1b), the maximal effect is 0.20 m in the spring and summer, and 0.17 meter in the autumn and winter of 2012. By stopping the extraction of Lonza industry, the groundwater level rises at VH45 (Scen 3a) between 0.57 - 1.55 meter. These are in between 0.28 – 0.89 in case the Lonza extractions are reduced for 50% (Scen 3b).

### 5.2 Additional scenarios

#### 5.2.1 Introduction

A set of additional scenarios have been formulated by Geotechnisches Institut AG and forwarded to Deltares on the 20<sup>th</sup> of August 2015 (reference 31.4426.001). Those scenarios are compared to the mean groundwater level at VH45 over the period 2<sup>nd</sup> of July 2012 and 16<sup>th</sup> of July 2012 for different adaptations of boundary conditions in the model. The adaptations are:

- N1. Side recharge from the mountains; all inflow around the entire model is reduced by 25% (multiplication with a factor 0.75) for the period 1<sup>st</sup> of January 2012 up to 31<sup>st</sup> of December 2012, see Figure 5.2-top;

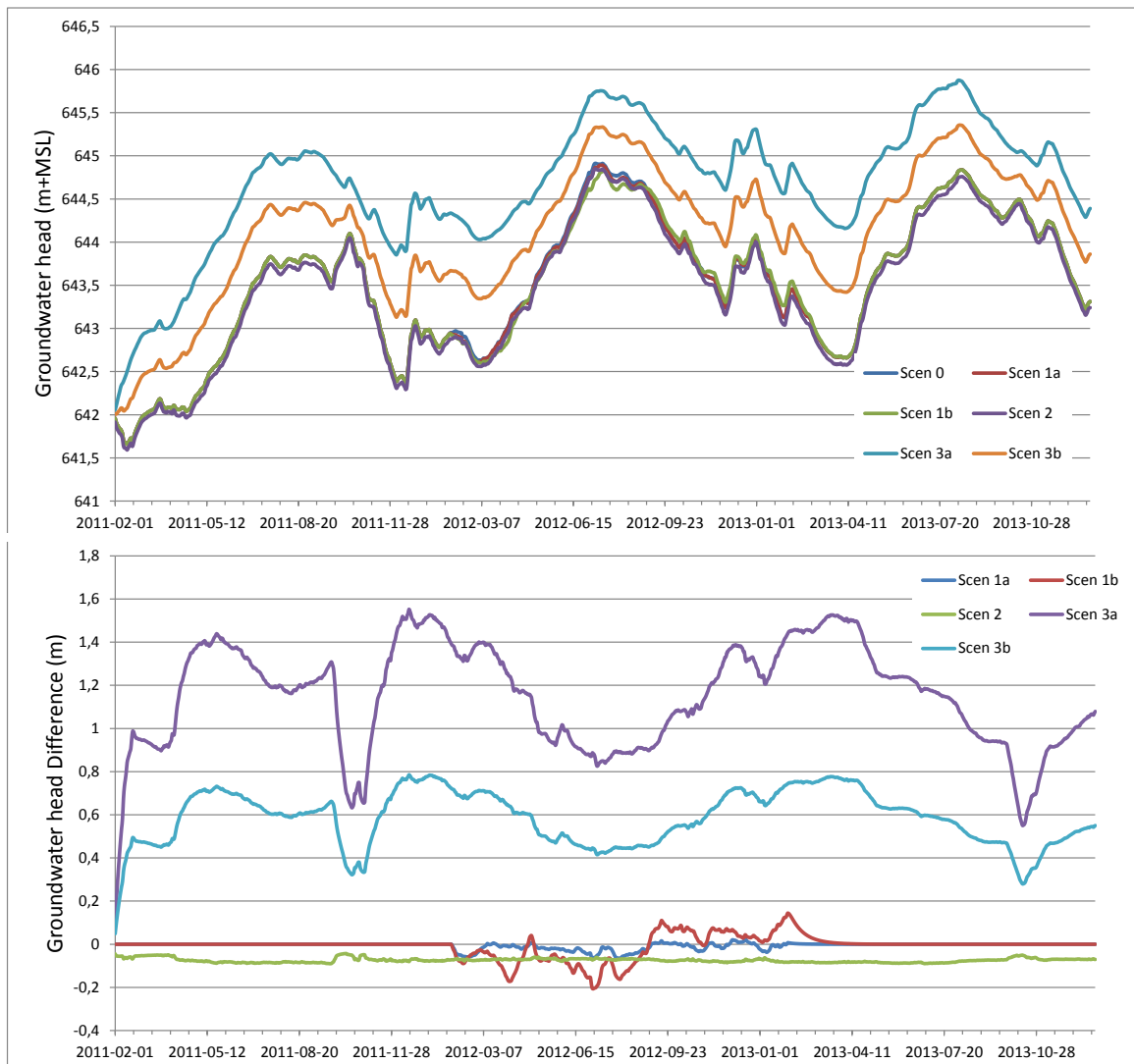


Figure 5.1 (top) Time series of the computed groundwater levels in VH45 in Visp; (bottom) the differences between the scenarios and the reference time series.

- N2. Side recharge from the mountains upstream of Katzenhaus; the inflow from the mountains is reduced for 50% (multiplication with a factor 0.50) for the period 1<sup>st</sup> of January 2012 up to 31<sup>st</sup> of December 2012, see Figure 5.2-bottom. The areas corresponds to the area 3 and 5 on Figure 3.8 on page 22;
- N3. Exchange of the Vispa River; the water levels from 2<sup>nd</sup> February 2011 up to the 31<sup>st</sup> of December 2011 were applied for the similar period in 2012 and applied for the Vispa River, see Figure 5.3-bottom. This scenario is equal to scenario 1a from section 5.1.1;
- N4. Exchange of the Rhône River; the water levels from 2<sup>nd</sup> February 2011 up to the 31<sup>st</sup> of December 2011 were applied for the similar period in 2012 and applied for the Rhône River, see Figure 5.3-top;
- N5. Drinking water Extraction; the extraction regimes for Hohbrunnen and Katzenhaus from 2nd February 2011 up to the 31st of December 2011 were applied to the similar period in 2012, see Figure 5.4-top.
- N6. Lonza Extraction; the extraction regime for Lonza from 2<sup>nd</sup> February 2011 up to the 31<sup>st</sup> of December 2011 were applied to the similar period in 2012, see Figure 5.4-bottom;



- N7. Inflow from the south; the groundwater levels are used from the 2<sup>nd</sup> of February 2011 up to the 31<sup>st</sup> of December 2011 for the similar period in 2012 and applied to the southern model boundary near Staldbach, see Figure 5.5-top;
- N8. Inflow from the east; the groundwater levels are used from the 2<sup>nd</sup> of February 2011 up to the 31<sup>st</sup> of December 2011 for the similar period in 2012 and applied to the eastern model boundary near Lalden, see Figure 5.5-bottom;

The adaptations of the model for the scenarios are depicted in the following figures.

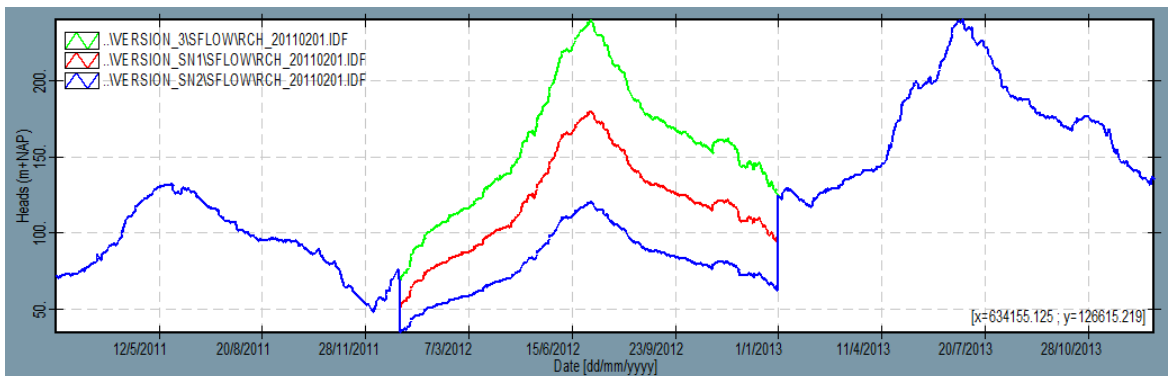


Figure 5.2 Side flow for (green) the original situation and (red) the scenario whereby this side flow is reduced for 75% and (blue) the situation whereby the side flow is reduced by 50% for the Vispa valley only.

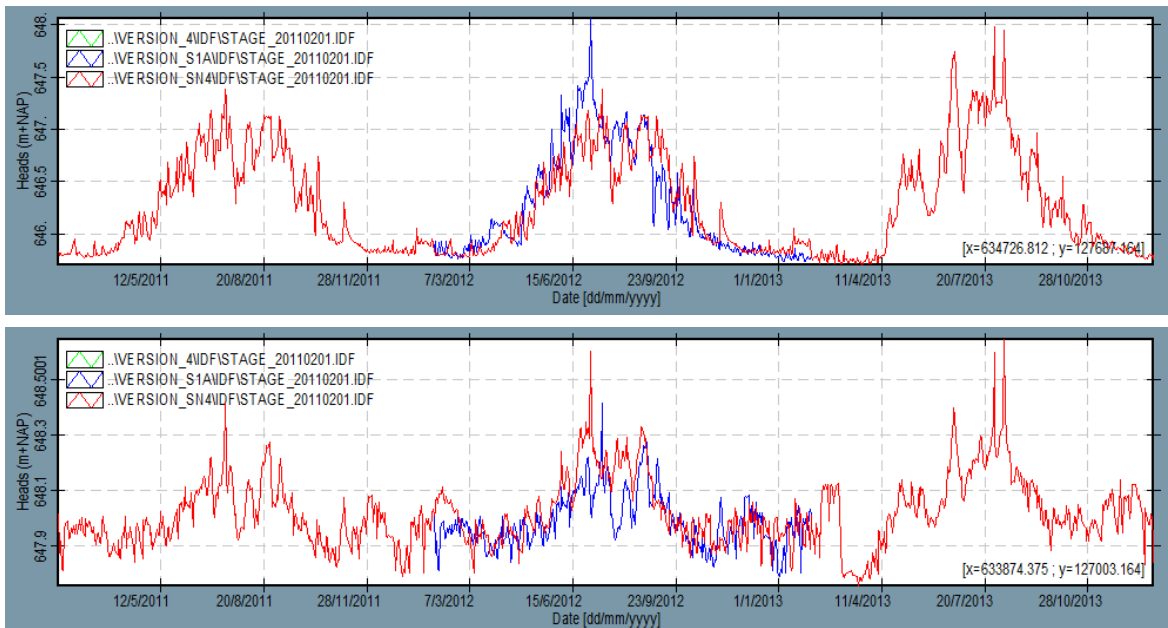


Figure 5.3 (top) The time series of the original river stage (blue) and 2011 sequence applied to 2012 for the Rhône and (bottom) the time series of the original river stage (red) and 2011 sequence applied to 2012 for the Vispa River (blue).

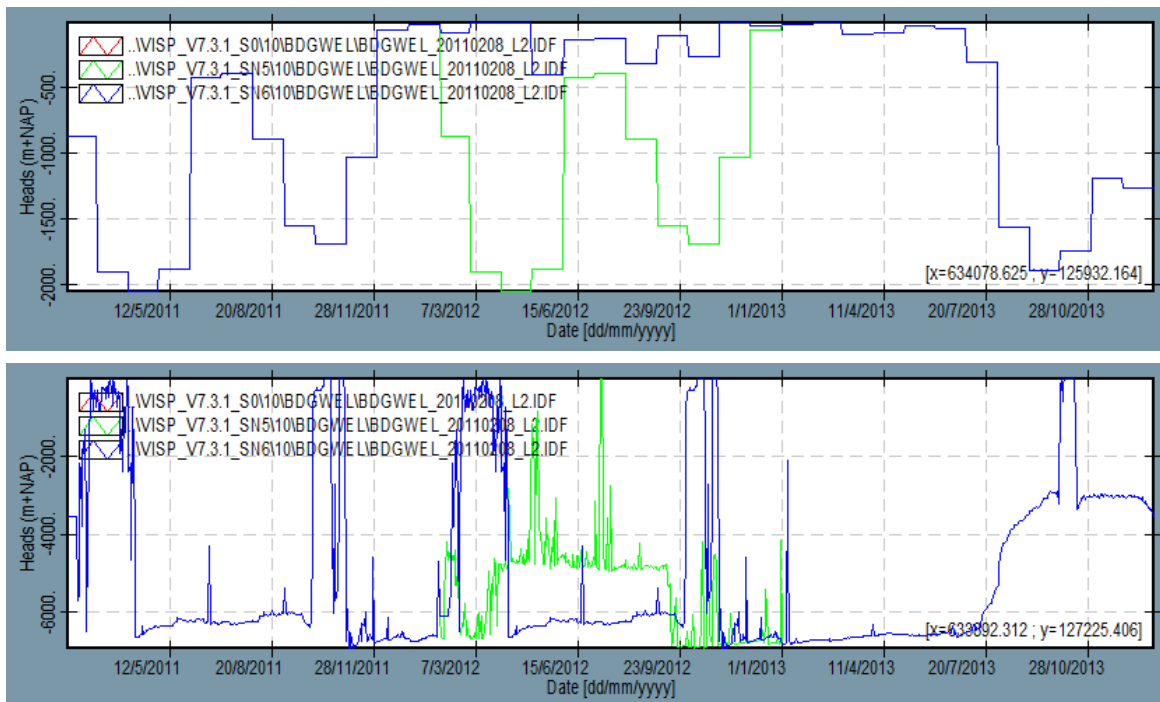


Figure 5.4 (top) time series of the (blue) original Hohbrunnen extraction and (green) the extraction regime of 2011 projected to 2012; (bottom) time series of the (green) original Lonza extraction (Sandmatten B1) and (blue) the extraction regime of 2011 projected to 2012.

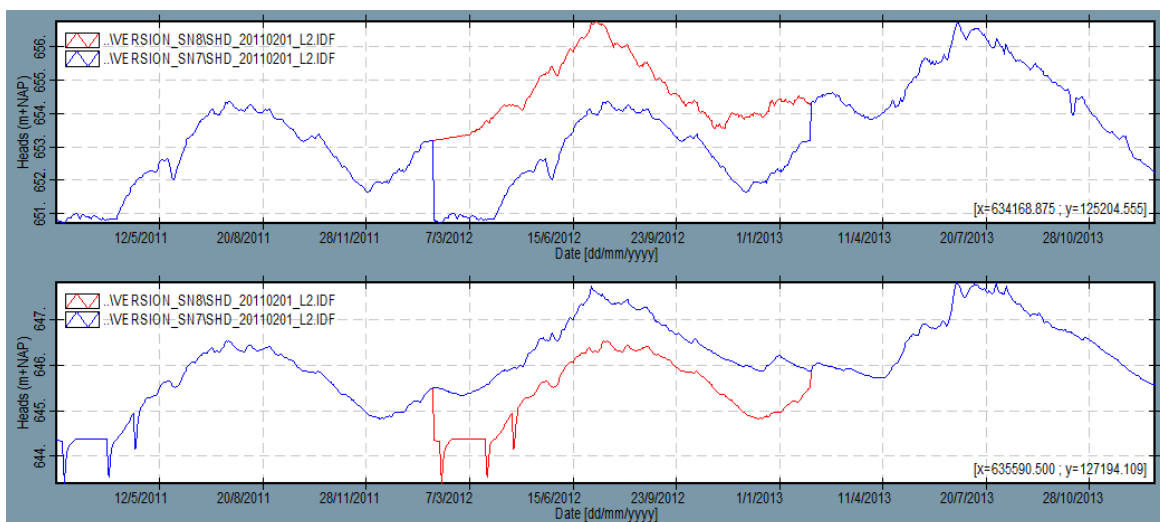


Figure 5.5 (top) time series of the (red) original groundwater level at Staldbach and (blue) the groundwater level of 2011 projected to 2012; (bottom) time series of the (blue) original groundwater level at Lalden and (red) the groundwater level of 2011 projected to 2012.

## 5.2.2 Results

The differences of the time series of the scenarios are given in Figure 5.6. From the figure it can be seen that the differences are positive and negative. The largest differences are caused by the Lonza extractions, positive during the spring and autumn and negative in the summer. According to 2011, Lonza extracted significantly less in summer. The drinking water extractions in the Vispa valley (Hohbrunnen and Katzenhaus) have an effect of maximal -0.18 m, though in the period 2<sup>nd</sup> of July up to the 16<sup>th</sup> of July 2012, the differences are negligible (-

0.01 m). The effects of the differences in water levels for the Vispa and Rhône Rivers are limited to -0.15 and +0.12 whereby the Rhône Rivers has a stronger influence than the Vispa River. The reduction of the side flow shows a more-or-less constant influence on the groundwater level of -0.08 m. The most influence is coming from the inflow in the Rhône valley from the east, more than 0.80 m. The extra inflow over the southern boundary inside the Vispatal is neglectable and less than 0.01m.

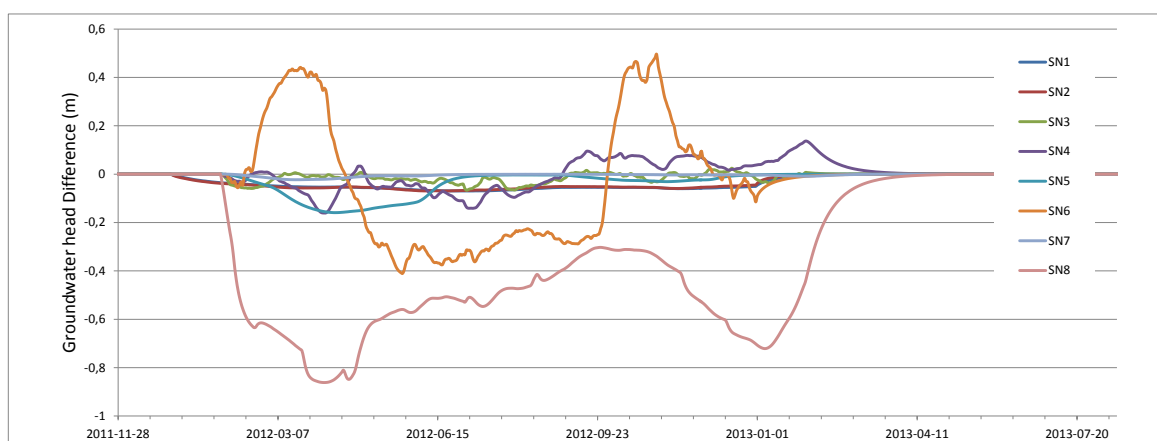


Figure 5.6 Simulated time series of the differences for the scenarios SN1 up to SN6.

The measured averaged head over the period 2<sup>nd</sup> of July 2012 and 16<sup>th</sup> of July 2012 is 645.06 m+MSL; the simulated averaged head is 644.88 m+MSL. The model simulated the groundwater head rather well. For this period, the differences by the various scenarios are presented in Table 5.1.

Table 5.1 Results for the additional scenarios.

Nr.	Simulation	Average groundwater at VH45 over the period 2 <sup>nd</sup> July 2012 – 16 <sup>th</sup> of July 2012		Difference (m)	Percent (%)
		Original	Scenario		
N1	Side recharge from mountains	644.88	644.81	-0.07	6.2
N2	Side recharge from the mountains upstream of Katzenhaus	644.88	644.81	-0.07	6.2
N3	Exchange of the Vispa River	644.88	644.83	-0.05	4.4
N4	Exchange of the Rhône River	644.88	644.75	-0.13	11.5
N5	Drinking water extraction Hohbrunnen/Katzenhaus	644.88	644.87	-0.01	0.9
N6	Lonza extraction	644.88	644.55	-0.33	29.2
N7	Groundwater levels at Staldbach	644.88	644.87	-0.01	0.9
N8	Groundwater levels at Lalden	644.88	644.35	-0.53	46.9
	Total drawdown (N1+N3+N4+N5+N6+N7+N8)			-1.13	100.0

It can be concluded that the groundwater level at VH45 is influenced by a variety of boundary conditions. Most important here are the Lonza and the inflow from the east at Lalden, they both summed up, take into account 75% of the altitude of the groundwater level at VH45.



## 6 Summary and recommendations

Since December 2011, the municipality of Visp, faces abnormally high groundwater levels. The authorities of Canton Valais together with the municipality of Visp have requested to study these extraordinary groundwater levels in the area of Visp. This report described the construction of a transient, three-dimensional groundwater flow model of the extended Visp basin and evaluated the effects of different boundary conditions around Visp, in relation to the groundwater observation in Visp (VH45). Based on the findings from this report the following results and recommendations can be made:

- 1 The quality of the model is good since it has been optimized thoroughly and carefully without adjusting parameters beyond their realistic bandwidth and has resulted in an average difference between the measured and observed groundwater levels of -0.03 meter (based on more than 4500 moment of observations). The computed groundwater levels show a realistic representation according to other field- and model studies applied earlier in the valley;
- 2 The average groundwater level in mid-July 2012 at VH45 (Visp) is strongly influenced by the inflow of groundwater from the east in the main Rhône valley. Almost 50% of the absolute groundwater level is determined by this inflow. The Lonza industry determines almost 30% of the altitude of the averaged groundwater level at VH45 in mid-July 2012, other minor boundary conditions are the water levels in the Rhône and Vispa Rivers (15%) and the side recharge from the mountains into the aquifers (5%);
- 3 The connection between the Rhône and Vispa valley results in an inflow of groundwater from a small valley into a wide valley. Since the Vispa valley is significantly shallower (approx. 100 meter depth) than the Rhône valley (approx. 1000 m depth), it yields a ratio of approx. 10%. From the simulations, it appeared that the groundwater level at VH45 (Visp) is influenced for 8% by boundary conditions from the Vispa valley. Within the Vispa valley itself, higher effects of groundwater level rise can occur since this narrow valley is more sensitive than a larger valley, such as the Rhône valley.





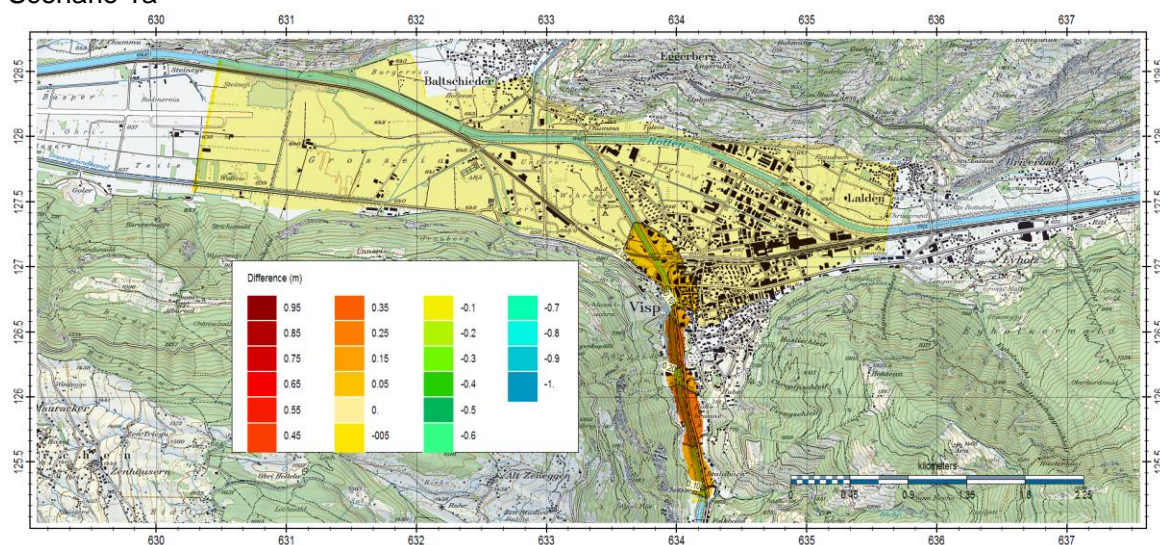
## 7 References

- Amt für Umwelt Kt. Solothurn: *Hydrogeologie Wasseramt*, 2008
- Besson, O., R. Marchant, A. Pugin, and J.-D. Rouiller, *Campagne de sismique-réflexion dans la vallée du Rhône entre Sion et St-Maurice: Perspectives d'exploitation géothermique des dépôts torrentiels sous-glaciaires*. Bulletin du Centre d'Hydrogéologie, Université de Neuchâtel, 1993. 12: p. 39 - 58.
- Borlat, C., *Troisième correction du Rhône, Modélisation 2d des écoulements, Souterrains dans la région de viègebaltschieder*, Faculty of Sciences Institute of Hydrogeology and Geothermics (CHYN), Université de Neuchâtel, 2012.
- Bundesamt für Umwelt BAFU, Rotten Flussvermessung, Messkampagne 122013, 2013.
- Bundesamt für Umwelt BAFU, *Flussvermessung Baltschiederbrücke-Susten*, 11-2010.
- Bundesamt für Umwelt BAFU, *Flussvermessung Vispa Rotten-Stalden*, 10-2010.
- Doherty, J., *Calibration and Uncertainty Analysis for Complex Environmental Models: PEST: complete theory and what it means for modelling the real world*, Watermark Numerical Computing, Brisbane, Australia, 2015.
- Geotechnisches Institut, *Grundwasserproblematik Visp: Detailuntersuchung Numerisches Grundwassermodell (reference 31.4426.001)*, from 27<sup>th</sup> of January 2015.
- Geotechnisches Institut, *Grundwasserproblematik Visp. Vertiefte statistische Auswertungen: Einfluss der Schneeschmelze und des Pegelstands der Vispa auf die GW-Stände in Visp (reference 31.4426.001)*, from 19<sup>th</sup> of June 2015.
- Glenz D., *Inverse Modeling of Groundwater flow in the Rhône Alluvial Aquifer, Impact of the third Rhône Correction*, Phd Thesis, Faculty of Sciences Institute of Hydrogeology and Geothermics (CHYN), Université de Neuchâtel, 2013.
- Fröhlich, A., *Etude de la variabilité spatiale des propriétés hydrogéologiques en milieu poreux hétérogène – Application à la vallée du Rhône entre Baltschieder et Gamsen (Valais)*. Travail de diplôme, Université de Neuchâtel, rapport et annexes, 1997
- Kimmeier, F., *3-D Groundwater Flow Modeling in Heterogeneous Geologic Media : Integrated Approach Using Spatial and Temporal Database, Geostatistics and GIS*. Thèse, Université de Neuchâtel, 2001.
- Rosseli, A. & Olivier, R. *Modélisation gravimétrique 2.5D et cartes des isohypses au 1:100'000 du substratum rocheux de la Vallée du Rhône entre Villeneuve et Brig (Suisse)*. Eclogae geol. Helv. 96 (2003)
- Vermeulen, P.T.M, and B. Minnema, 2015. *iMOD user manual*. Version: 3.01, July 2015. Deltares, The Netherlands. (<http://oss.deltares.nl/web/iMOD>).
- WEA, Kt. Bern: *Nutzungs-, Schutz- und Überwachungskonzept für den Grundwasserleiter des Seelands*, Schlussbericht. 1999.
- WEA, Kt. Bern: *Hydrogeologie Seeland*, Stand 2004
- Swiss Seismological Service, *COGEAR-Project*, 2015 (<http://www.cces.ethz.ch/projects/hazri/COGEAR>).

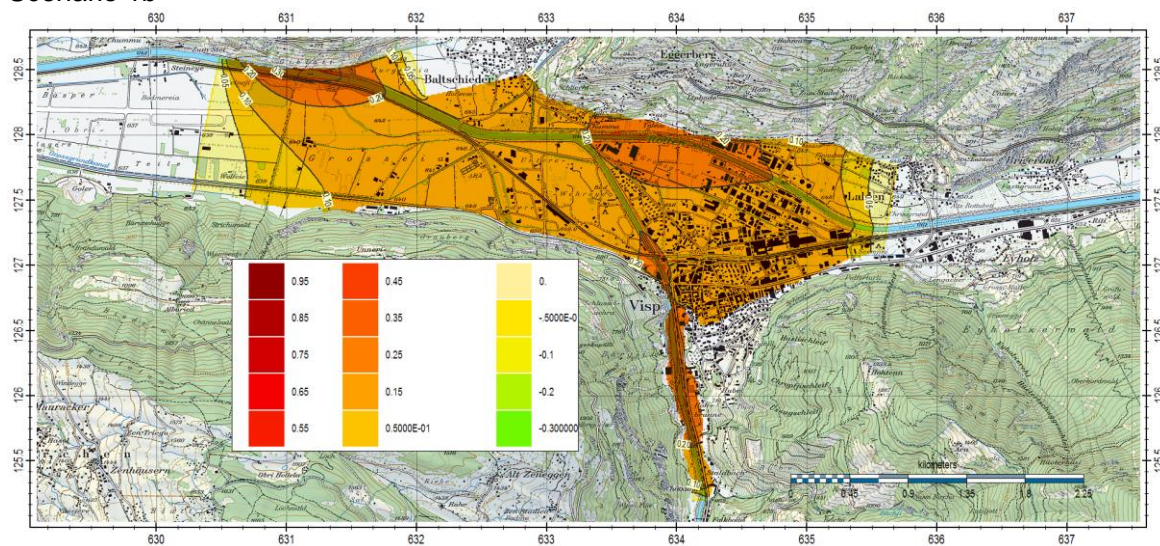


## A Drawdown of Scenarios

Scenario 1a

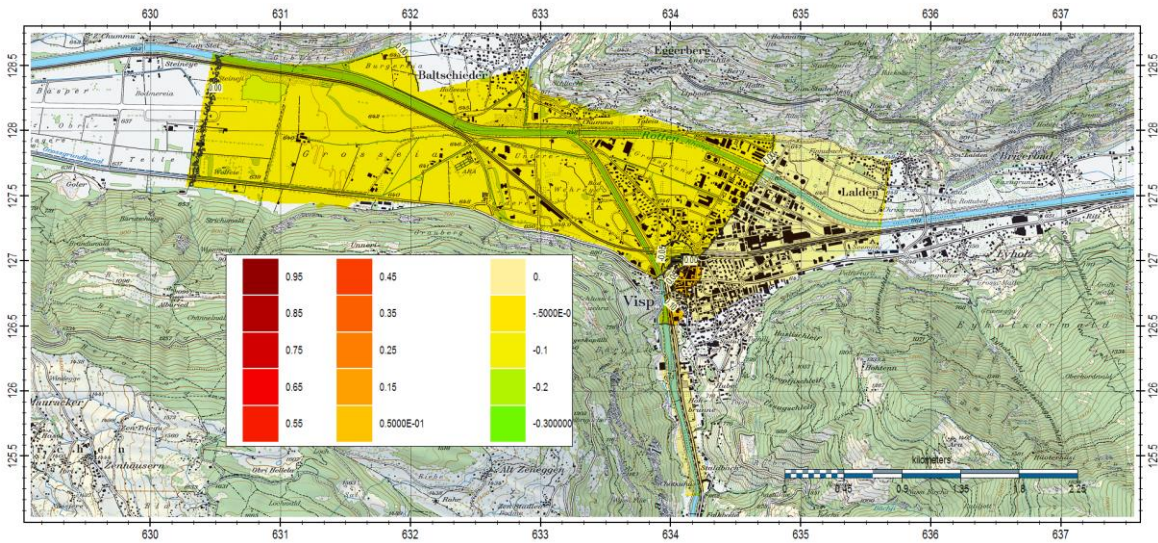


Scenario 1b

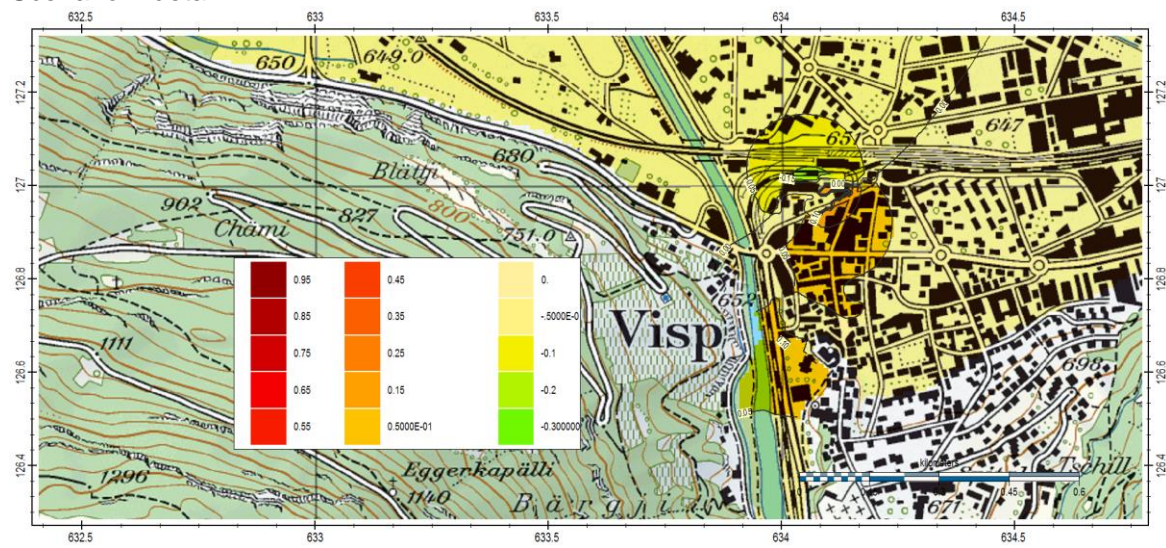




## Scenario 2

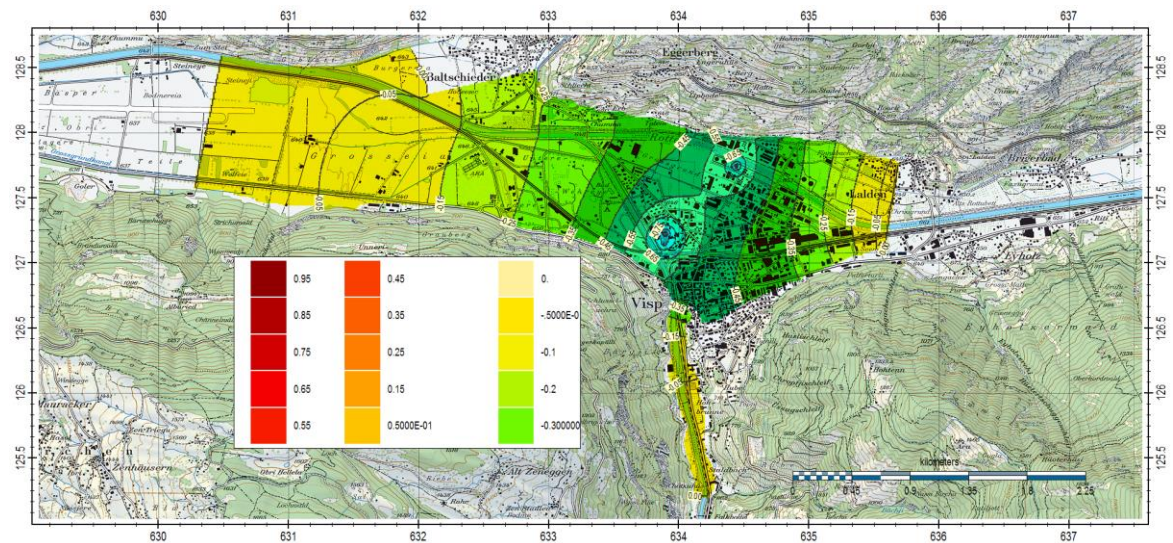


## Scenario 2 detail





Scenario 3a



Scenario 3b

